International Journal of Electrochemical Science 19 (2024) 100873

Contents lists available at ScienceDirect

International Journal of Electrochemical Science

journal homepage: www.editorialmanager.com/ijoes

Evaluation of 14-(p-tolyl)-14H-dibenzo[*a,j*]xanthene as a highly efficient organic corrosion inhibitor for mild steel in 1 M HCl: Electrochemical, theoretical, and surface characterization

Azzeddine Belkheiri [a], Khadija Dahmani [b], Mohamed Khattabi [a], Khaoula Mzioud [a], Otmane Kharbouch [a], Mouhsine Galai [a,*], Nadia Dkhireche [a], Zakaria Benzekri [b,c], Said Boukhris [b], Rafa Almeer [d], Basheer M. Al-Maswari [e], Mohamed Ebn Touhami [a]

[a] *Advanced Materials and Process Engineering, Faculty of Sciences, Ibn Tofaïl University, PO Box 133, Kenitra 14000, Morocco*
[b] *Laboratory of Organic, Inorganic Chemistry, Electrochemistry and Environment, Faculty of Sciences, Ibn Tofaïl University, PO Box 133, Kenitra 14000, Morocco*
[c] *Laboratory of Heterocyclic Organic Chemistry, Department of Chemistry, Faculty of Sciences, Mohammed V University in Rabat, Rabat BP 1014, Morocco*
[d] *Department of Zoology, College of Science, King Saud University, P.O. Box 2455, Riyadh 11451, Saudi Arabia*
[e] *Department of Chemistry, Yuvaraja's College, University of Mysore, Manasagangotri, Mysuru 570 006, India*

A R T I C L E I N F O

Keywords:
Mild steel
Corrosion inhibition
HCl
Density functional theory

A B S T R A C T

Corrosion of mild steel, particularly in acidic environments such as hydrochloric acid (HCl), remains a critical issue due to its impact on material durability, economic costs, and safety concerns. This study introduces 14-(p-tolyl)-14H-dibenzo[*a,j*]xanthene (ZM5), a novel and highly effective organic corrosion inhibitor, to mitigate this challenge. Employing advanced electrochemical techniques: electrochemical impedance spectroscopy (EIS) and potentiodynamic polarization (PDP), we evaluated ZM5's performance in a 1 M HCl solution, revealing an impressive inhibition efficiency of 94.7 %. Surface characterization using scanning electron microscopy (SEM) and energy-dispersive X-ray spectroscopy (EDX) further confirmed the formation of a robust protective film on the steel surface, shedding light on ZM5's adsorption mechanisms. Complementing the experimental findings, Density Functional Theory (DFT) simulations provided theoretical insights into the anti-corrosion mechanism of ZM5, aligning well with observed results. These findings underscore ZM5's potential as a highly promising corrosion inhibitor for industrial applications, effectively enhancing the corrosion resistance of mild steel in aggressive environments.

1. Introduction

Metals are integral to numerous industries due to their exceptional mechanical properties and ease of processing [1]. Their superior performance makes them essential in applications ranging from structural components to advanced technology [2–4]. Despite their advantages, metals are susceptible to environmental degradation, which can lead to significant economic losses and reduced material lifespan [5].

Among these metals, mild steel (MS), characterized by a carbon content below 0.25 %, is widely utilized due to its favorable properties, including high strength, good ductility, and cost-effectiveness[6]. Its machinability and robust performance make it a material of choice for applications such as pipelines, plates, and structural beams in sectors including construction, automotive manufacturing, and petrochemicals [7–9].

However, mild steel is particularly vulnerable to corrosion, especially when exposed to acidic environments such as hydrochloric acid used in cleaning and pickling processes. This susceptibility is further exacerbated in humid or chlorinated environments, presenting both safety hazards and increased costs [6,10]. It is estimated that approximately 30 % of metallic equipment and materials are discarded annually due to corrosion, leading to significant resource waste and elevated risk factors [7,11,12].

The investigation of mild steel corrosion in acidic environments has become a focal point for research due to the increasing use of acidic solutions in industrial processes such as acid cleaning, oil well acidification, and petrochemical operations [1].

To mitigate corrosion, various strategies are employed, including

* Corresponding author.
E-mail addresses: galaimouhsine@gmail.com (M. Galai), ralmeer@ksu.edu.sa (R. Almeer).

https://doi.org/10.1016/j.ijoes.2024.100873
Received 27 September 2024; Received in revised form 9 November 2024; Accepted 9 November 2024
Available online 12 November 2024

electroplating, electrochemical protection, coatings, and the application of corrosion inhibitors [13–15]. Among these methods, the use of corrosion inhibitors is particularly advantageous due to its cost-effectiveness, high efficacy, and practicality [16–19].

Recent research has focused on identifying organic compounds that can effectively inhibit corrosion in highly acidic environments [20,21]. The most effective inhibitors often feature aromatic rings and atoms of nitrogen, sulfur, and oxygen [22–27]. Research shows that organic heterocyclic compounds with conjugated double bonds, polar functional groups, and electronegative atoms are particularly promising as synthetic corrosion inhibitors [7,28–31]. For instance, inhibitors incorporating heterocyclic structures and functional groups, such as nitrogen, sulfur, and oxygen, have demonstrated substantial protection against corrosion in acidic environments, as evidenced by recent studies [32–35]. These compounds often exhibit high adsorption efficiency on metal surfaces, leading to the formation of protective films that significantly reduce corrosion rates [36,37]. The studies highlighted earlier showcase the effectiveness of various synthesized inhibitors, confirming their ability to inhibit steel corrosion in hydrochloric acid through mechanisms consistent with the Langmuir adsorption isotherm [38,39]. This underscores the potential for further exploration and development of organic corrosion inhibitors in industrial applications.

In this context, ZM5 is introduced as a novel corrosion inhibitor for mild steel in a 1 M HCl solution, aiming to address limitations observed with existing inhibitors. The choice of ZM5 is based on its unique molecular structure, which includes polar functional groups and large electronegative atoms known to enhance adsorption on the steel surface and promote protective film formation. Unlike conventional inhibitors, ZM5 is designed to provide stronger adsorption and improved inhibition efficiency, even in challenging acidic conditions. This study will evaluate the efficacy of ZM5 using advanced electrochemical techniques, including electrochemical impedance spectroscopy (EIS) and potentiodynamic polarization (PD). Detailed surface characterization will be conducted using scanning electron microscopy (SEM) and energy-dispersive X-ray spectroscopy (EDX) to analyze adsorption mechanisms and the formation of protective films.Table 1.

This table shows that **ZM5 achieves a high inhibition efficiency of 94.7 %**, which is competitive or superior to other commonly studied inhibitors. Its high efficiency, even at relatively low concentrations, highlights its potential as an effective corrosion inhibitor for mild steel in acidic environments. The presence of nitrogen and sulfur in ZM5's structure appears to enhance adsorption on the steel surface, forming a protective layer that inhibits corrosion effectively.

2. Experimentation

2.1. Materials and sample preparation

The corrosive environment for the study was created by preparing a 1.0 M HCl solution from a 37 % hydrochloric acid, which was diluted with distilled water. The mild steel samples used for this investigation were meticulously prepared to ensure accurate results. Their composition is carbon (C) 0.11 %, silicon (Si) 0.24 %, manganese (Mn) 0.47 %, chromium (Cr) 0.12 %, molybdenum (Mo) 0.02 %, nickel (Ni) 0.1 %, aluminum (Al) 0.03 %, copper (Cu) 0.14 %, cobalt (Co) <0.0012 %, vanadium (V) <0.003 %, tungsten (W) 0.06 %, with the balance being iron (Fe). To prepare the specimens, they were subjected to mechanical abrasion using progressively finer grades of emery paper (From 80–2000), followed by thorough washing, degreasing, and drying in ambient air. This preparation ensured that the samples were in optimal condition for evaluating the corrosion inhibition performance of the ZM5 inhibitor. The inhibitor solutions were tested across a concentration range from 10^{-3} M to 10^{-6} M, and a control solution was also prepared for comparative analysis. Our inhibitor ZM5 was dissolved in dimethyl sulfoxide (DMSO) to ensure complete solubility and optimal availability for interaction with the metal surface. DMSO was chosen due to its effectiveness in dissolving organic compounds, which aids in achieving uniform distribution of the inhibitor in solution. Scheme 1 presents the molecular structures of ZM5.

Table1
Comparison of corrosion inhibition efficiency of various organic compounds.

Compound	Concentration	Inhibition Efficiency (%)	Ref.
ZM5	10^{-3} M	**94.7**	*This study*
Imidazole derivative	10^{-3} M	92.5	[40]
Thiazole derivative	5×10^{-4} M	92.11	[41]
Benzotriazole derivative	100 PPM	80	[42]
Pyridine-based compound	10^{-3}	85.4	[43]
Quinoline derivative	2 %	84.23	[44]
Thiourea-based compound	2×10^{-4} M	87.0	[45]
Schiff base	200 ppm	91.06	[46]
Piperidine derivative	10^{-3}	84.5	[47]

2.2. General procedure for preparation of 14-(4-methyl phenyl)-14H-dibenzo [a,j] xanthene derivatives

A mixture of 2-naphtol (2.0 mmol), 4-methyl phenyl (1.0 mmol), and SnP_2O_7 catalyst (2.5 mol%) in 3 mL of ethanol was refluxed. The progress of reactions was monitored by TLC. After completing the reaction (as confirmed by TLC), the reaction mixture was mixed with 3 mL of hot ethanol for dilution. The catalyst, which was insoluble in this solvent, was then separated from the reaction mixture using filtration through fritted glass. The separated catalyst underwent two washes with 3 mL portions of ethanol each. It was subsequently dried under vacuum at 100 ∘C and made ready for use in the next run. Following the catalyst separation, the solvent obtained from the separation process was evaporated, resulting in a precipitate. This precipitate was subjected to recrystallization from hot ethanol to obtain the pure compound. The structure of this layer was confirmed by appropriate spectroscopic and physical methods (Melting point, ^{1}H NMR and ^{13}C NMR), the spectral data given below [48].

^{1}H NMR ($CDCl_3$, 300 MHz) δ ppm: 8.38–7.78 (m, 6 H), 7.58–7.55 (m, 2 H), 7.46 (d, J =8.7 Hz, 2 H), 7.42–7.39 (m, 4 H), 6.93 (d, J =8.0 Hz, 2 H), 6.46 (s, 1 H), 2.12 (s, 3 H). 13 C NMR ($CDCl_3$, 75 MHz) δ ppm: 148.73, 142.12, 135.85, 131.47, 131.02, 129.11, 128.78, 128.70, 128.08, 126.75, 124.22, 125.20, 122.60, 118.06, 117.44, 37.61, 20.72.

2.3. Electrochemical analysis

The electrochemical analysis was conducted using Voltamaster software in conjunction with a PGZ 100 potentiostat, focusing on two

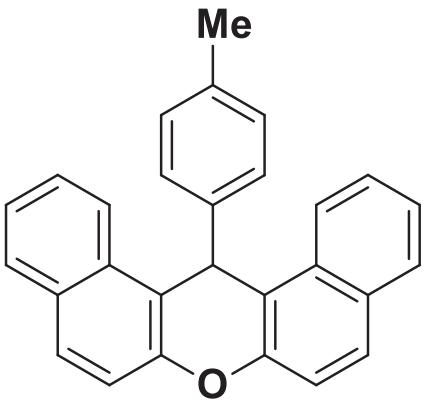

Scheme 1. molecular structures of 14-(p-tolyl)-14H-dibenzo[*a,j*]xanthene (ZM5).

key methodologies: Electrochemical Impedance Spectroscopy (EIS) and Potentiodynamic Polarization (PP). These methods were employed to evaluate the corrosion behavior of mild steel in 1 M hydrochloric acid (HCl) solutions, both with and without corrosion inhibitors. The steel samples were first rinsed with distilled water to eliminate any loose debris. They were then polished using different grades of abrasive paper, ranging from 180 to 1200 grit, to achieve a clean, smooth surface. After polishing, the samples were rinsed again with distilled water to remove any residues from the polishing process,in addition,the working electrode was immersed in the test solution for 30 minutes to allow the establishment of a stable open circuit potential (OCP), after which the electrochemical measurements were initiated.

For EIS measurements, an alternating current (AC) signal with an amplitude of 10 mV was used, covering a frequency range from 100 kHz to 100 mHz. Concurrently, potentiodynamic polarization curves were obtained over a potential range from −900 mV to −100 mV/SCE with a scan rate of 1 mV/s. All experiments, except for those investigating temperature effects, were performed under standard atmospheric conditions, with the mild steel sample's exposed surface area consistently set at 1 cm^2. Data analysis and curve fitting were carried out using EC-Lab software, which models the data with an analog electrical circuit. Temperature effects were studied over a range from 298 K to 328 K.

2.4. Surface characterization

To elucidate the surface alterations of steel subjected to hydrochloric acid, both with and without the studied inhibitors, a detailed examination was performed using scanning electron microscopy (SEM) combined with energy dispersive X-ray (EDX) analysis. Steel specimens were exposed to 1 M HCl solutions for 6 hours, under conditions with and without the inhibitors.

2.5. Computational methods and definitions

2.5.1. Gaussian calculations

Gaussian 09 package program was used to the study of the isolated compounds using density functional theory (DFT), with the B3LYP functional [49] under the 6–31 G (d, p) basis sets. GaussView 6.0 program was employed to prepare the correlative calculation parameters for the compounds under probe. As we all know, electrochemical corrosion generally happens in liquid environment. One of the most popular approaches to research solvent effect is to consider hydrogen bonded clusters of solvent molecules surrounding the solute molecules. Thus self-consistent reaction field (SCRF) theory, with Tomas's polarized continuum model (PCM) [50] was used to describe the solvent effect of water. This method describes the solvent as a structureless continuum with uniform dielectric permittivity, in which a molecular-shaped empty cavity is dug to host the solute [51]. The reliability of PCM method to explore the solvent effect in the field of corrosion inhibitors has been validated by many researchers [52–54].

2.5.2. Quantum global chemical reactivity

We also calculated various structural indices, such as the load distribution, molecular orbital energies E_{HOMO} and E_{LUMO}, and the dipole moment(μ). These parameters were then utilized to estimate key electronic properties, including the energy gap (ΔEgap), total hardness (η), softness (σ), electronegativity (χ), and the number of electrons transferred (ΔN) from the inhibiting molecule to the metal atom. Additionally, we computed the electrophilicity (ω), nucleophilicity (ε), electronic back-donation energy (ΔE_{b-d}), the electronic charge-accepting capability, and the initial molecule-metal interaction energy $(\Delta\psi)$. These quantities were determined using global hardness (η) and electronegativity (χ) as outlined in Eqs. (6–8) [55,56].

$$\Delta E_{gap} = E_{LUMO} - E_{HOMO} \tag{1}$$

$$\eta_{Inh} = \frac{[E_{LUMO} - E_{HOMO}]}{2} = \frac{\Delta E_{gap}}{2} \tag{2}$$

$$\sigma = \frac{1}{\eta} \tag{3}$$

$$\chi_{Inh} = -\left(\frac{E_{LUMO} + E_{HOMO}}{2}\right) \tag{4}$$

$$\omega_{Inh} = \frac{\chi_{Inh}^2}{2\eta_{Inh}} \tag{5}$$

$$\varepsilon_{Inh} = \frac{1}{\omega_{Inh}}$$

$$\Delta N = \frac{\phi - \chi_{Inh}}{2(\eta_{Fe} + \eta_{Inh})} \tag{6}$$

$$\Delta E_{back-donation} = \frac{-\eta}{4} \tag{7}$$

$$\Delta\psi = -\frac{(\chi_{Fe} - \chi_{Inh})^2}{4(\eta_{Fe} + \eta_{Inh})} \tag{8}$$

Where ϕ is the work function used as a measure of the electronegativity of iron. The value of $\phi = 4.82$ eV for the Fe (110) surface, which is reported to have higher stabilization energy [57]. We adopted a theoretical value of $\chi_{Fe} = 7.0eV$ $and \eta_{Fe} = 0$ based on the assumption that for metallic bulk, $I = A$ (ionization potential equals electron affinity), since metallic bulk is softer than neutral metallic atoms [55].

2.5.3. Fukui indices and dual Fukui descriptors

Nucleophilic/electrophilic sites for ZM5 molecular structures were estimated by Fukui functions. The equations used to identify electrophilic attack sites (f_k^-), nucleophilic attack sites (f_k^+), free radical attack sites (f_k^0), local softness (σ_k^α) and local electrophilicity (ω_k^α) were presented in Eqs. 10–14 [58,59].

$$f_k^+ = q_k(N+1) - q_k(N) \tag{9}$$

$$f_k^- = q_k(N) - q_k(N-1) \tag{10}$$

$$f_k^0 = \frac{q_k(N+1) - q_k(N-1)}{2} \tag{11}$$

$$\sigma_k^\alpha = \sigma f_k^\alpha \tag{12}$$

$$\omega_k^\alpha = \omega f_k^\alpha \tag{13}$$

In which $q_k(N), q_k(N+1) and q_k(N-1)$ are the electron population of atom k in the neutral, anionic, and cationic molecules, respectively. The values of $\alpha = -, 0 and +$ represent the local softness values describing, electrophilic, radical, and nucleophilic attacks, respectively. Specifically, the double Fukui descriptor or second order Fukui functions f_k^2, the related dual local softness $\Delta\sigma_k$ and the dual local philicity $\Delta\omega_k$ are employed to provide a simple and instinctive insight into local chemical reactivity. These double descriptors are defined in the following way:

$$\Delta f_k = f_k^+ - f_k^- \tag{14}$$

$$\Delta\sigma_k = \sigma_k^+ - \sigma_k^- \tag{15}$$

$$\Delta\omega_k = \omega_k^+ - \omega_k^- \tag{16}$$

3. Results and discussions

3.1. Concentration effect

3.1.1. Open circuit potential (OCP)

Fig. 1 shows the evolution of the open circuit potential (OCP) of mild steel in 1 M HCl solution with different concentrations of the inhibitor ZM5

The curves show that the addition of ZM5 results in a shift towards more positive potentials, indicating a reduction in corrosion. As ZM5 concentration increases, this shift becomes more pronounced, indicating better protection. At low concentrations of 10–6 M and 10–5 M, the effect is less pronounced but remains higher than the control without inhibitor[60]. After 1800 s, the potential stabilizes, suggesting an equilibrium between the metal surface and the corrosive medium. These results confirm that ZM5 improves the corrosion resistance of mild steel in acidic environments, with greater effectiveness at higher concentrations.

3.1.2. PDP test

In the context of potentiodynamic polarization (PDP) analysis, the polarization curves provide critical insights into the corrosion behavior of mild steel in the presence and absence of the inhibitor ZM5 in a 1 M HCl solution.

From the polarization curves shown in Fig. 2, it is evident that the addition of ZM5 affects both anodic and cathodic branches of the polarization plots. The anodic curve demonstrates a notable reduction in current density when ZM5 is present, indicating that the inhibitor significantly impedes the anodic dissolution of iron, which is primarily associated with the oxidation process. This suggests that ZM5 exerts a strong inhibitory effect on the anodic reaction, thereby reducing the overall corrosion rate. Moreover, the cathodic curve is shifted toward lower current densities, albeit less pronounced than the anodic shift. This shift implies that ZM5 also hinders the hydrogen evolution reaction to some extent, albeit its primary action appears to be on the anodic process. The fact that both anodic and cathodic currents are reduced suggests that ZM5 acts as a mixed-type inhibitor, affecting both anodic and cathodic reactions to a certain degree, though its primary influence is on the anodic mechanism.

The electrochemical parameters summarized in Table 2 provide a clear view of how the ZM5 inhibitor affects mild steel corrosion at different concentrations. As shown, the corrosion current density (i_{corr}) decreases markedly with increasing ZM5 concentration. Specifically,

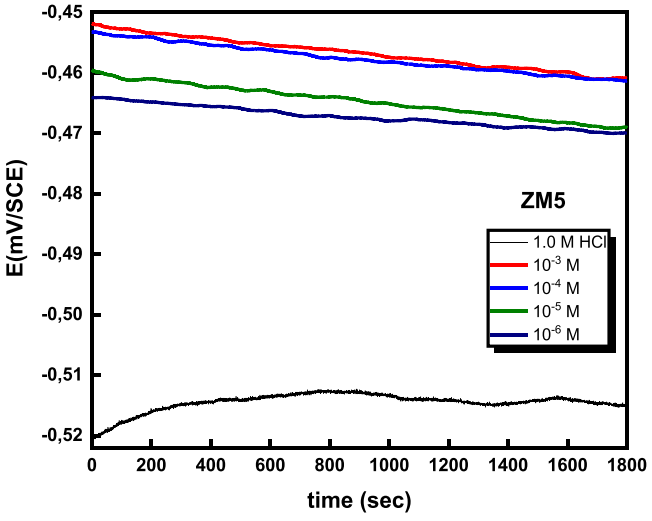

Fig. 1. Variation of Open Circuit Potential (OCP) Over Time for Mild Steel in 1.0 M HCl with ZM5 at Different Concentrations.

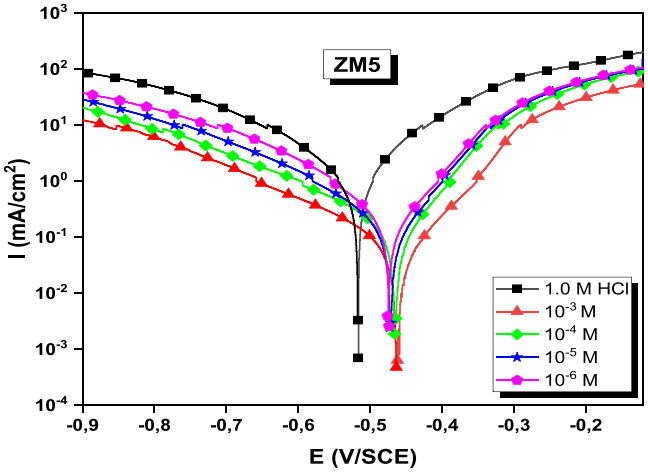

Fig. 2. Polarization curves for mild steel immersed in 1 M HCl solution, in the absence and presence of different concentrations of ZM5, at a temperature of 298 K.

Table 2
corrosion parameters determined by PDP of mild steel in 1.0 M HCl without and with ZM5 at 298 K.

	C (mol/L)	-E_{corr} mV/SCE	i_{corr} μA.cm^{-2}	-β_c mV dec^{-1}	β_a mV dec^{-1}	η_{PP} %
Blank	–	515	1045	133	134	–
ZM5	10^{-6}	469	190	127	121	81.8
	10^{-5}	469	118	124	133	88.8
	10^{-4}	461	80	119	128	92.3
	10^{-3}	460	55	131	125	94.7

icorr drops from 515 μA/cm^2 in the uninhibited solution to 55 μA/cm^2 at a concentration of 10^{-3} mol/L, indicating a substantial inhibition of corrosion. This trend suggests that higher concentrations of ZM5 enhance its adsorption onto the steel surface, forming a protective barrier that effectively limits both iron dissolution and hydrogen ion reduction. The interaction likely involves the electron-rich heteroatoms (N and O) and the π-electrons in the benzene rings of ZM5, which creates a stable complex on the metal surface, blocking active sites responsible for corrosion. En ce qui concerne la variation du potentiel de corrosion (Ecorr), on observe une légère déviation vers des valeurs plus positives avec l′ajout de ZM5, mais le décalage reste inférieur à 85 mV par rapport à l′échantillon sans inhibiteur. Cela suggère queue ZM5 agit comme un inhibiteur mixte sans effet de polarisation préférentiel, affectant à la fois les processus anodiques et cathodiques. Cependant, la légère augmentation de Ecorr pourrait indiquer une inhibition plus marquée du processus anodique.

The anodic (βa) and cathodic (βc) Tafel slopes also show significant variations with the addition of ZM5. The decrease in βc with increasing ZM5 concentration indicates a reduction in the cathodic hydrogen reduction reaction, although less pronounced than the anodic inhibition. Similarly, the slight variation in βa suggests that the inhibitor also affects the anodic dissolution process. These variations in βa and βc confirm that ZM5 influences both reactions but has a greater affinity for suppressing iron dissolution, supporting its role as a mixed-type inhibitor with an anodic tendency. The inhibition efficiency (ηPP) reaches 94.7 % at the highest concentration of 10^{-3} mol/L, confirming the increasing effectiveness of ZM5 as a corrosion inhibitor through adsorption on the metal surface.

3.1.3. EIS test

EIS (Electrochemical Impedance Spectroscopy) is a crucial tool in corrosion studies, providing valuable insights into inhibition

mechanisms, particularly through the analysis of Nyquist and Bode plots, which represent impedance and phase angle over a broad frequency range, respectively. Fig. 3 shows that in a 1 M HCl solution at 298 K, whether inhibited or not, the Nyquist plots display a single, distorted capacitive arc, indicative of the double layer capacitance at the metal/solution interface [7,61].

As the concentration of ZM5 increases, both the size of this capacitive arc and the impedance values rise, indicating enhanced resistance to electrochemical reactions and thus a more effective corrosion inhibition [21]. The addition of the ZM5 inhibitor significantly reduces the corrosion rate of mild steel, as evidenced by changes in the phase angle and impedance spectra [25,62]. These changes are attributed to the formation of a protective layer at the metal/solution interface, confirming that the ZM5 inhibitor plays a crucial role in establishing this protective barrier against corrosion [17,23].

Additionally, the phase angle spectra (Fig. 5) consistently display a single peak across all experimental conditions, suggesting the presence of a single time constant for the corrosion process at the interface[63]. The phase angle peaks, consistently below 90°, are likely attributed to surface roughness and metal non-uniformity in a real system [63,64]. As the concentration of ZM5 increases, both the phase angle peak and its half-width also increase, reflecting an expansion of the interfacial layer, a decrease in the double layer capacitance, and an extension of the frequency response time [65,66].

This behavior can be attributed to the gradual replacement of water molecules adsorbed on the metal surface by organic inhibitor molecules. At higher concentrations of ZM5, the adsorption of these molecules becomes more pronounced, reducing the exposed surface area to corrosion, increasing the thickness of the double layer, and lowering the local dielectric constant [67]. Furthermore, the increase in the low-frequency impedance modulus, as shown in Fig. 3, indicates a rise in charge transfer resistance, thereby enhancing the effectiveness of ZM5 in corrosion protection [18,21,28].

The electrochemical parameters obtained through the modeling of spectra using an electrical circuit are illustrated in Fig. 6.

The results in Table 3 confirm a strong correlation between the effectiveness of the inhibitors and the findings obtained using the PDP method.

The addition of the ZM5 inhibitor results in a significant increase in charge transfer resistance (R_{ct}), as evidenced by the rise in R_{ct} values and the decrease in double layer capacitance (C_{dl}) with increasing doses of ZM5 [68,69]. These data support the conclusion that the ZM5 molecule induces changes at the metal/corrosive medium interface through adsorption [70].

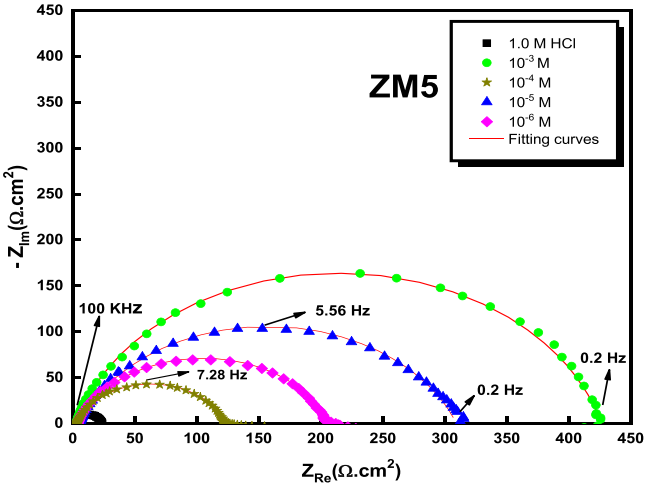

Fig. 3. Effect of ZM5 concentrations on Nyquist diagrams of mild steel in 1.0 M HCl solution.

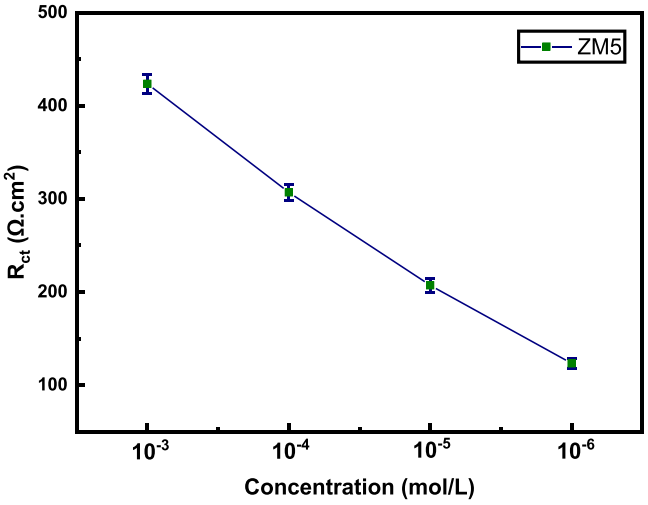

Fig. 4. Variation of Rct with ZM5 concentration, including error bars.

The electrochemical behavior observed in the EIS measurements indicates that the ZM5 inhibitor enhances corrosion protection primarily by modifying the charge transfer resistance (R_{ct}) and double layer capacitance (C_{dl}) at the metal interface. The single capacitive arc in the Nyquist plots suggests a predominantly charge-transfer-controlled process at the mild steel surface. As the concentration of ZM5 increases, the larger R_{ct} values, along with the lower C_{dl} values, imply an effective barrier against charge transfer, indicative of a stable inhibitor layer. Additionally, the Bode plots show a rise in the impedance modulus at low frequencies, which points to the inhibitor's efficiency in enhancing resistance to corrosive reactions. The consistent single-time-constant behavior in phase angle spectra supports the formation of a homogenous protective layer that limits the diffusion of corrosive species to the metal surface.

Specifically, the decrease in the values of the proportional constant (Q) in the presence of inhibitors, compared to the uninhibited medium, suggests the formation of an insulating layer on the surface of the mild steel [71]. In parallel, the increase in the CPE (n) exponent observed for the inhibitor reflects an increased surface inhomogeneity due to adsorption, which reduces the active surface area exposed to corrosion [12].

3.2. *Temperature effect*

Temperature has a significant influence on the behavior of materials in corrosive environments, as shown in previous research. To further investigate this influence, a potentiodynamic study was carried out to evaluate the effect of temperature variation on inhibition efficiency. The study examined the system both with and without the ZM5 inhibitor, across a temperature range from 298 K to 328 K. The results, presented in Fig. 7, were analyzed to extract key electrochemical parameters, which are summarized in Table 3.

The data shown in Fig. 7 and Table 4 clearly demonstrate that increasing temperature results in higher current densities across all scenarios, irrespective of whether inhibitors are present. This indicates that temperature influences corrosion rates by diminishing the effectiveness of inhibition. For instance, the inhibition efficiency decreases by 91.1 %. Notably, the polarization curves with and without ZM5 remain parallel, suggesting that temperature does not affect the underlying protection mechanism, as previously discussed [9]. This finding supports the idea that higher temperatures enhance the desorption of adsorbed molecules.

Despite this, Table 4 reveals a consistent decrease in inhibition efficiency with rising temperatures, indicating that the inhibitor remains strongly adsorbed on the metal surface even at elevated temperatures.

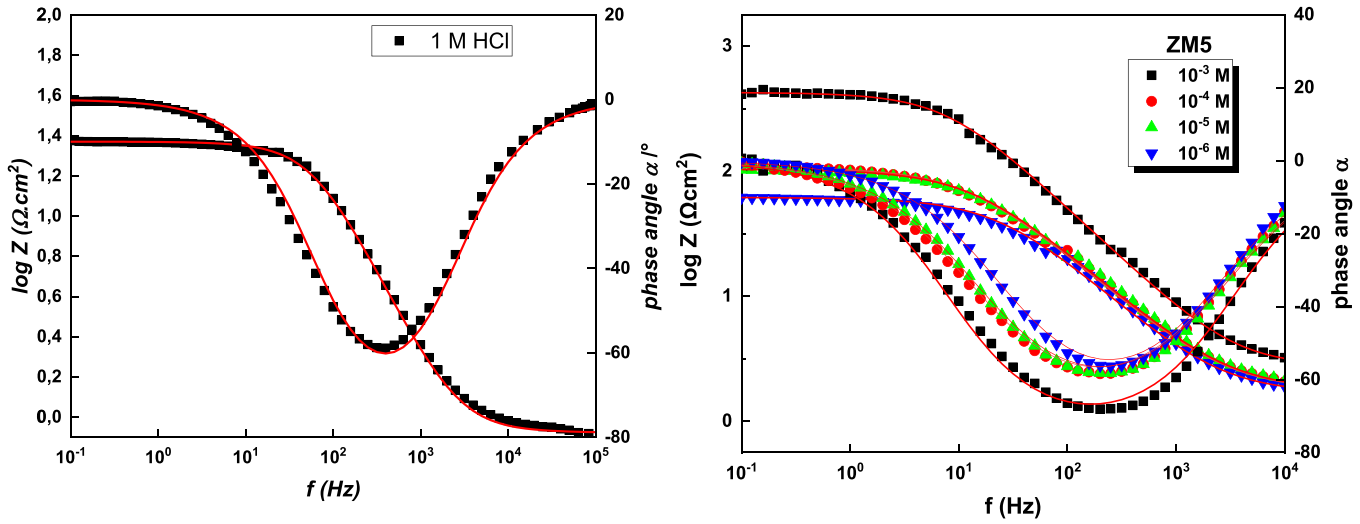

Fig. 5. Bode diagrams for mild steel with and without variation of ZM5 concentrations in 1.0 M HCl solution.

Fig. 6. Equivalent circuits compatible with experimental impedance data.

This suggests a physisorption mechanism for the molecules on the metal surface, corroborating results from earlier studies [72–74].

To further substantiate these observations, activation parameters are analyzed and calculated using the following equations [75]:

$$Lni_{corr} = LnA - \frac{E_a}{RT} \tag{19}$$

$$Ln\left(\frac{I_{corr}}{T}\right) = \left(Ln\left(\frac{R}{Nh}\right) + \frac{\Delta Sa}{R}\right) - \frac{\Delta Ha}{RT} \tag{20}$$

Table 5 provides a summary of these activation parameters.

Analysis of the data (Table 5) reveals a significant increase in activation energy E_a, rising from 28.7 kJ/mol in the absence of ZM5 to 34.1 kJ/mol with its presence. This elevation in activation energy indicates that the inhibitor contributes to creating an additional energy

Table 3
Electrochemical parameter values for mild steel in 1.0 M HCl solution with varying concentrations of ZM5.

	C (mol/L)	R_s (Ω.cm²)	Q (μF.S^{n-1})	n	C_{dl} (μF cm^{-2})	R_{ct} (Ω.cm²)	X^2 (10^{-4})	θ	*SD* (Ω.cm²)	η_{imp} %
Blank	–	0.8	211	0.9	133.0	22.7	2.2	–	1.2	–
ZM5	10^{-6}	1.66	312.5	0.77	115.1	123.3	4.2	0.816	5.1	81.6
	10^{-5}	1.76	303.2	0.79	106.9	207.1	5.9	0.890	7.2	89.0
	10^{-4}	1.74	294.8	0.77	106.5	306.9	6.3	0.926	8.5	92.6
	10^{-3}	2.72	88	0.84	46.6	423.5	2.7	0.946	10.3	94.6

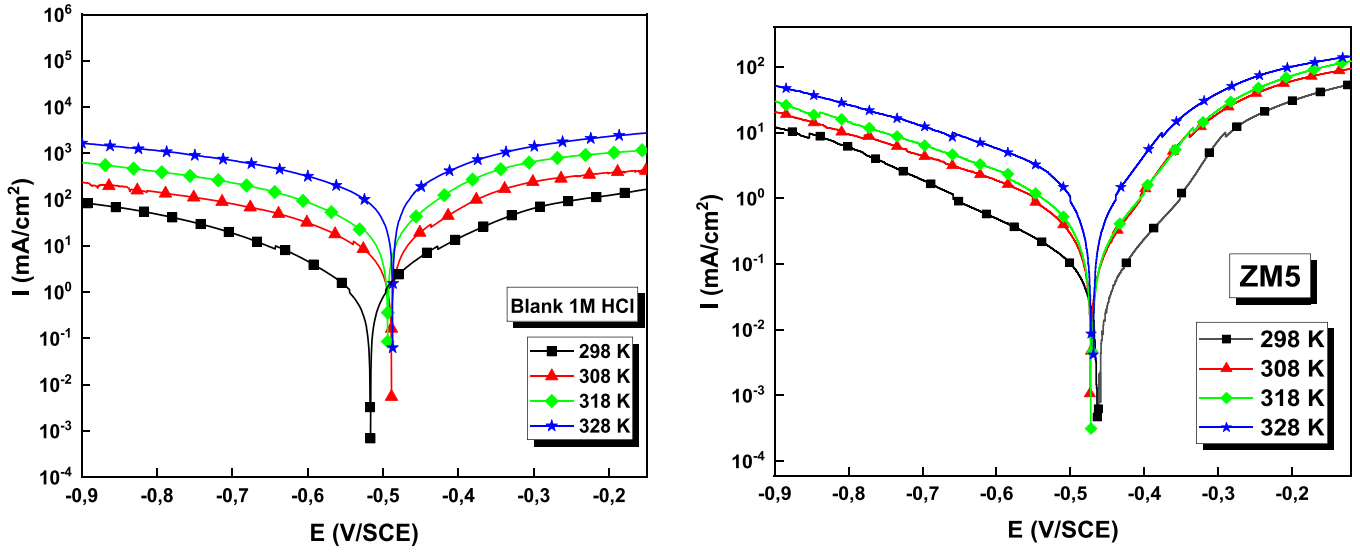

Fig. 7. Potentiodynamic polarization plots for MS in 1.0 M HCl with 10^{-3} M ZM5 at different temperatures.

Table 4
The electrochemical factors of mild steel at the optimum concentration of ZM5 in the temperature range of 298–328 K.

	T	$-E_{corr}$ (mV_{SCE})	i_{corr} ($\mu A/cm^2$)	$-\beta_c$ (mV/dec)	β_a (mV/dec)	η_{pp} (%)
Blank	298	515	1045	133	134	–
	308	487	1644	186	110	–
	318	491	2069	162	118	–
	328	486	3150	153	114	–
ZM5	298	460	55	131	125	94.7
	308	468	110	179	103	93.3
	318	469	166	158	117	92.0
	328	468	281	143	110	91.1

Table 5
Thermodynamic parameters of the inhibition study in the presence and absence of ZM5.

	E_a (kJ/mol)	ΔH_a (kJ/mol)	ΔS_a (J/mol.K)
Blank	28.7	26.2	−99.2
ZM5	34.1	40.5	−75.2

barrier for the corrosion reaction [62]. In other words, the presence of ZM5 appears to promote the formation of a protective interface on the mild steel surface, making metal dissolution more difficult. This result also suggests that the inhibitor modifies the corrosion mechanism, requiring greater energy input to initiate the reaction [76]. In addition, the positive values observed for activation enthalpy (ΔH_a), increasing from 26.2 kJ/mol without the inhibitor to 40.5 kJ/mol with ZM5, indicate an endothermic process during metal dissolution [77,78]. This suggests that the corrosion reaction, in the presence of the inhibitor, necessitates additional energy input. A higher activation enthalpy indicates that the interactions between the metal and ZM5 are sufficiently strong to significantly influence the corrosion mechanism, thereby reinforcing the idea that the inhibitor acts to stabilize the metal surface. Regarding activation entropy, the observed values show a significant increase, changing from −99.2 J/mol·K without the inhibitor to −75.2 J/mol·K in the presence of ZM5. This variation indicates a greater disorder in the system during the adsorption of the inhibitor. This change in entropy may be attributed to the displacement of water molecules adsorbed on the metal surface during interaction with ZM5 [79,80]. The increased order of the adsorbed inhibitor molecules on the metal surface also contributes to enhanced stability of the formed inhibitive interface, which is essential for protection against corrosion.

3.3. Adsorption isotherms

Understanding the adsorption process is essential for evaluating the performance of corrosion inhibitors, as it sheds light on their mechanisms of action. To characterize these interactions, adsorption isotherms such as Langmuir, Temkin, and Freundlich are frequently employed [81]. In this study, we utilized the Langmuir isotherm model to analyze the adsorption behavior of the ZM5 molecule.

Fig. 9 demonstrates a perfect linear relationship ($R^2 = 1$) between the concentration C and C/θ, which validates the suitability of the Langmuir model for accurately depicting the adsorption process [27]. This finding is significant as it validates the use of Langmuir isotherms to characterize the interactions between the inhibitor and the metal surface. The physical significance of the Langmuir isotherm lies in its representation of the adsorption process as a dynamic equilibrium between the adsorption and desorption of molecules on a solid surface. It assumes that the surface consists of a finite number of identical sites, where each site can only hold one adsorbate molecule, leading to monolayer coverage. This model highlights that the rate of adsorption is proportional to the concentration of the adsorbate in the solution and reflects the saturation point at which no further adsorption can occur once all sites are occupied. Additionally, the Langmuir isotherm implies that the interactions between adsorbate molecules do not affect one another, simplifying the understanding of surface coverage dynamics. Overall,

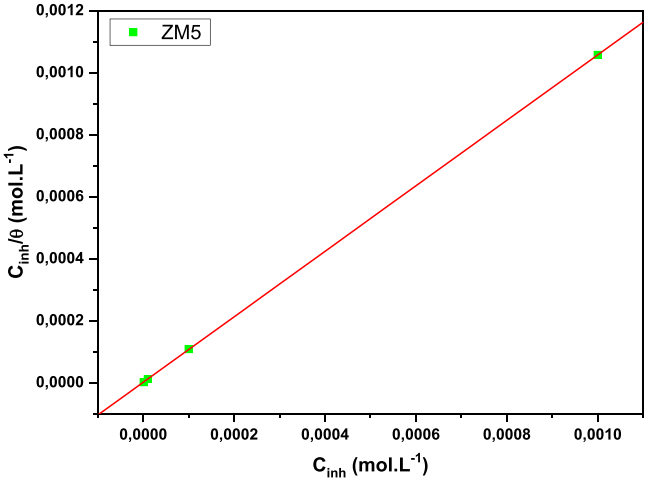

Fig. 9. Langmuir adsorption isotherm for mild steel in 1.0 M HCl with ZM5.

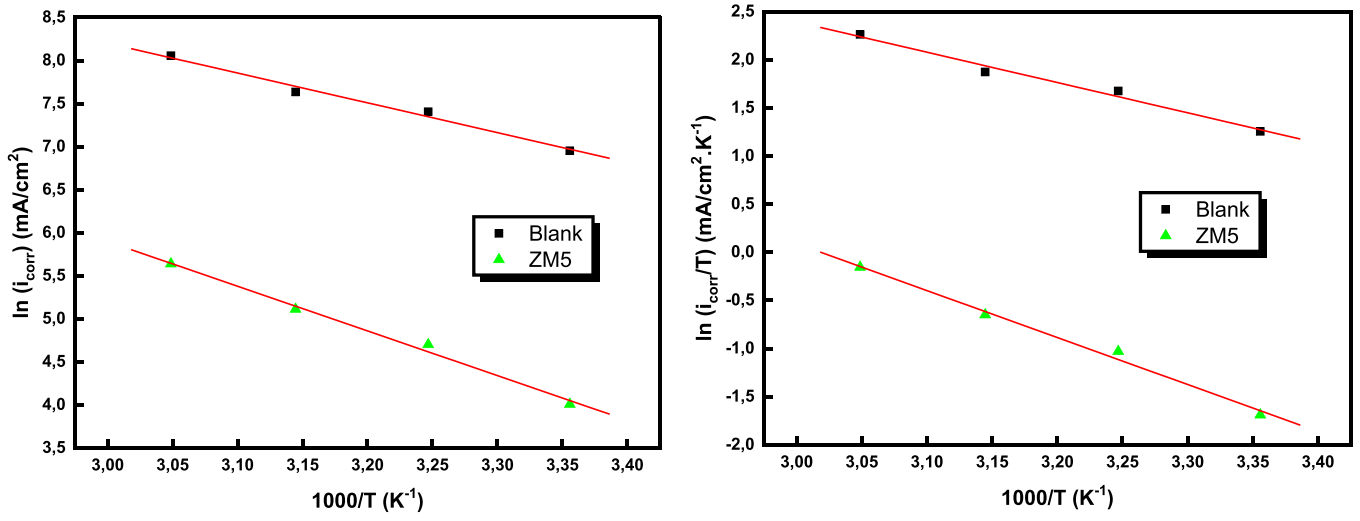

Fig. 8. Arrhenius and Transition State Plots for mild steel corrosion in 1.0 M HCl with and without 10^{-3} M ZM5.

this model provides crucial insights into the efficiency and mechanisms of corrosion inhibitors, such as ZM5, in forming protective layers on metal surfaces.

The corresponding adsorption isotherm can be expressed using the following formula[20,60]:

$$\frac{\theta}{1-\theta} = K_{ads} \times C \tag{21}$$

In these formulas, C represents the concentration of the corrosion inhibitor, θ indicates the surface coverage, and K_{ads} is the adsorption equilibrium constant. These parameters are detailed in Table 6.

The standard Gibbs free energy of adsorption ΔGads is an important thermodynamic parameter that can be derived from the adsorption constant K_{ads} using the equation provided Eq. 22.

$$\Delta G_{ads} = -RTln(55.5K_{ads}) \tag{22}$$

For the ZM5 molecule, the Gibbs free energy of adsorption ΔGads is calculated to be −44.1 kJ/mol. This value, being below −40 kJ/mol, indicates that the adsorption is likely chemical in nature, as such low values typically denote strong, specific interactions characteristic of chemical adsorption [82].

Furthermore, the high adsorption equilibrium constant K_{ads} underscores the strong affinity of ZM5 for the metal surface. This significant K_{ads} value reflects the efficient adsorption of ZM5, forming a highly stable protective layer[83]. The consistency between the Gibbs free energy and K_{ads} values supports the conclusion that ZM5 inhibits corrosion effectively through robust chemical bonding.

3.4. Scanning electron microscopy with energy dispersive spectroscopy

The surfaces of metal specimens soaked in 1 M HCl for 6 h were examined using SEM-EDS analysis. Fig. 10 shows the SEM images and corresponding EDS spectra in both the presence and absence of ZM5. The SEM images reveal that the metal surface immersed in the blank solution suffers from extensive damage and corrosion, with an unstable layer of corrosion products forming. After the introduction of ZM5, the mild steel surface shows significantly less deterioration, displaying a smoother surface with no corrosion around small defects. This suggests that ZM5 forms a protective layer on the steel surface, providing strong inhibition by effectively shielding the metal from the corrosive effects of the acidic environment.

The EDS analysis of the polished mild steel surfaces highlights peaks corresponding to the main elements on the metal. The detection of nitrogen in the blank solution could be attributed to exposure to air. When ZM5 is present, the nitrogen content on the surface increases noticeably, suggesting that ZM5 molecules, which contain nitrogen, adsorb onto the metal surface. At the same time, the oxygen content is significantly reduced, indicating that ZM5 blocks active adsorption sites, thereby hindering the corrosion process.

3.5. Computational methods and definitions

3.5.1. Global reactivity descriptors

The optimized electronic structures correspond to energy minima without imaginary frequencies. According to frontier molecular orbital theory and in agreement with Fukui theory, a high E_{HOMO} value indicates a molecule's ability to donate electrons to a designated acceptor (in this case, the metal surface) with an empty molecular orbital, facilitating the adsorption process and thus reflecting good inhibitory performance [84]. In contrast,E_{LUMO} is associated with electron affinity, reflecting a tendency to accept electrons. Therefore, the molecular energy gap is a key descriptor to calculate. It demonstrates the inherent ability to donate electrons and evaluates the interaction between inhibitor molecules and the substrate surface. The optimized molecular structures, HOMO, LUMO, and the molecular electrostatic potential of the studied molecules are shown in Fig. 11.

Several studies [85,86] have reported that the inhibition efficiency of inhibitors is correlated with various quantum chemical parameters such as η,σ,χ and dipole moment (DM). Additionally, descriptors like ω (electrophilicity index), ε (energy), ΔN (fraction of electrons transferred), ΔE_{b-d} (binding energy), and $\Delta\psi$ (interaction energy), calculated based on η and χ, are also highly useful in corrosion inhibition studies of organic molecules[87]. The quantum chemical parameters we calculated for the inhibitor molecule in both the gas phase and aqueous phase are presented in Tables 7and 8.

The quantum chemical analysis of the ZM5 compound reveals its significant potential as an effective corrosion inhibitor in both gas and aqueous environments. The HOMO energy values of −5.472 eV (gas phase) and −5.665 eV (aqueous phase) indicate that ZM5 is a strong electron donor, capable of transferring electrons to the metal surface during adsorption, which is essential for the inhibition process. The LUMO energy values (-1.106 eV in gas, −1.289 eV in aqueous) further highlight ZM5's ability to accept electrons, making it versatile in its interactions with the metal surface. A critical parameter, the HOMO-LUMO energy gap is relatively small in both environments (4.366 eV in gas, 4.376 eV in aqueous), demonstrating that ZM5 is a soft molecule. This small energy gap suggests that the compound has high reactivity, facilitating efficient electron transfer between the inhibitor and the metal, which plays a vital role in mitigating corrosion [88]. A molecule with a small energy gap is more easily polarizable, enabling it to adapt to surface interactions, which is crucial for adsorption and protective film formation. The electronegativity (χ) values of 3.289 eV (gas) and 3.477 eV (aqueous) indicate that ZM5 has a moderate tendency to attract electrons. In combination with its relatively low hardness ($\eta = 2.183eV\ in\ gas\ and 2.188eV\ in\ aqueous$), ZM5 emerges as a reactive species with a balanced ability to both donate and accept electrons, further enhancing its inhibition performance.

The softness ($\sigma = 0.4581eV^{-1} in\ gas\ and 0.457\ eV^{-1} in\ aqueous$) confirms the molecule's high reactivity and adaptability in various environments, making it effective in both gas and aqueous phases [89]. The electrophilicity index (ω) values suggest that ZM5 is also a moderately good electron acceptor. This enhances its capability to interact with metal surfaces by accepting electron density from the metal during adsorption, stabilizing the surface-inhibitor interaction. In contrast, the nucleophilicity index (ϵ), which is the inverse of electrophilicity, shows that ZM5 is also a strong electron donor, especially in the gas phase, reinforcing its dual role in electron transfer processes during corrosion inhibition [90].

The total energy values of ZM5 in the gas phase and aqueous phase indicate that the compound is slightly more stable in the aqueous environment. This added stability in water, combined with its enhanced electrophilicity and electron-donating capabilities, suggests that ZM5 will perform particularly well in aqueous environments where corrosion is typically more aggressive. In conclusion, the quantum chemical parameters, including a small energy gap, high softness, balanced electrophilicity and nucleophilicity, and low hardness, all point to ZM5 being a highly efficient corrosion inhibitor. Its ability to efficiently donate and accept electrons ensures strong interactions with the metal surface, contributing to the formation of a protective layer that prevents further corrosion. The molecule has enhanced stability and reactivity in aqueous environments further support its application in environments where corrosion is a significant concern, making ZM5 a promising candidate for corrosion inhibition.

Table 7 provides a comprehensive analysis of the quantum chemical properties of the ZM5 compound in both gas and aqueous phases, crucial for understanding its corrosion inhibition potential. The calculated

Table 6
Adsorption parameters from studied isotherm.

Inhibitor	K_{ads} (L/mol)	$-\Delta G_{ads}$ (kJ/mol)	R^2
ZM5	972006.2	44.1	1

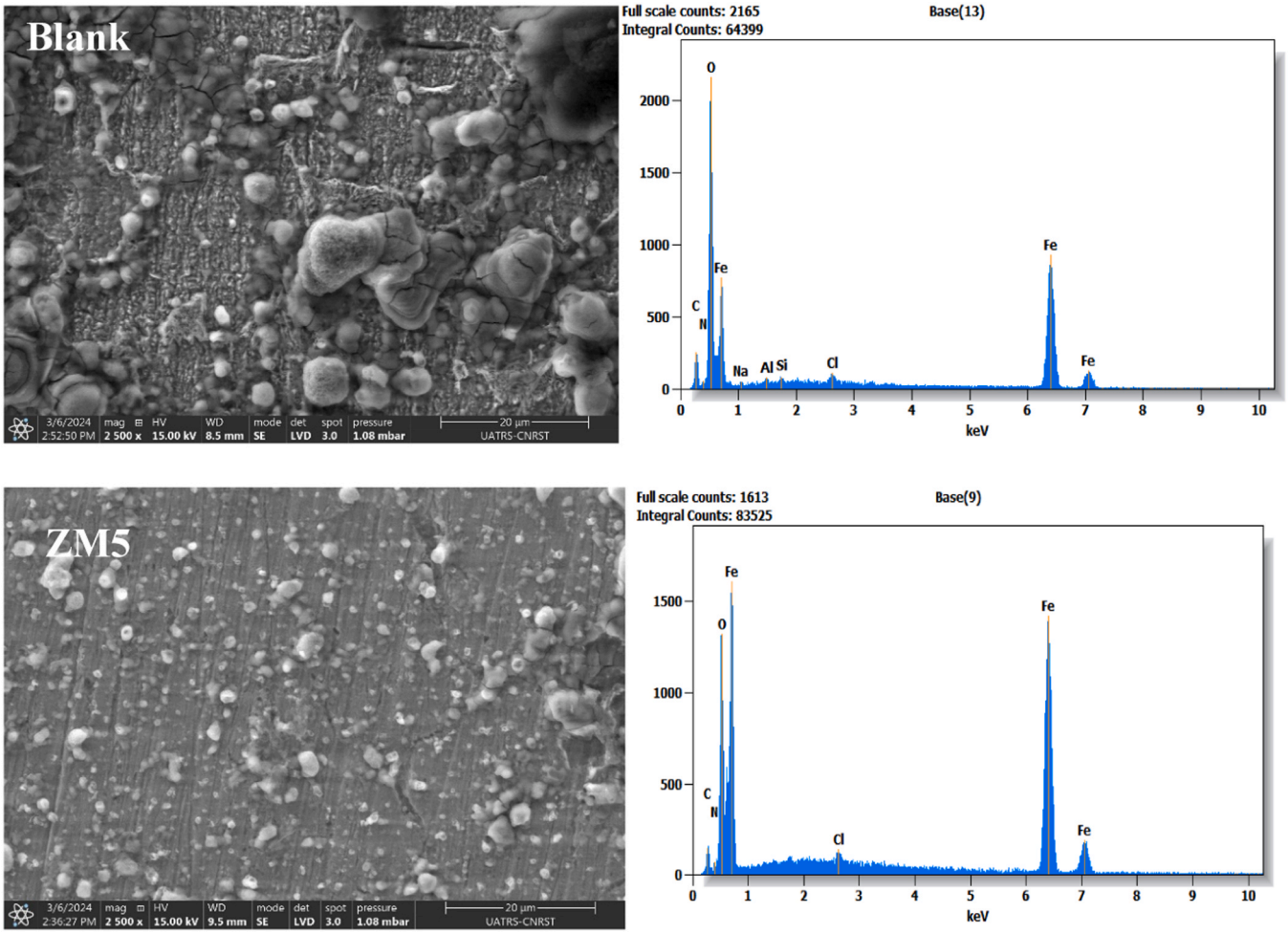

Fig. 10. SEM microscopy and EDX spectra obtained for mild steel surface pre and post 6 hour immersion in 1.0 M HCl solution, with and without ZM5, at 298 K.

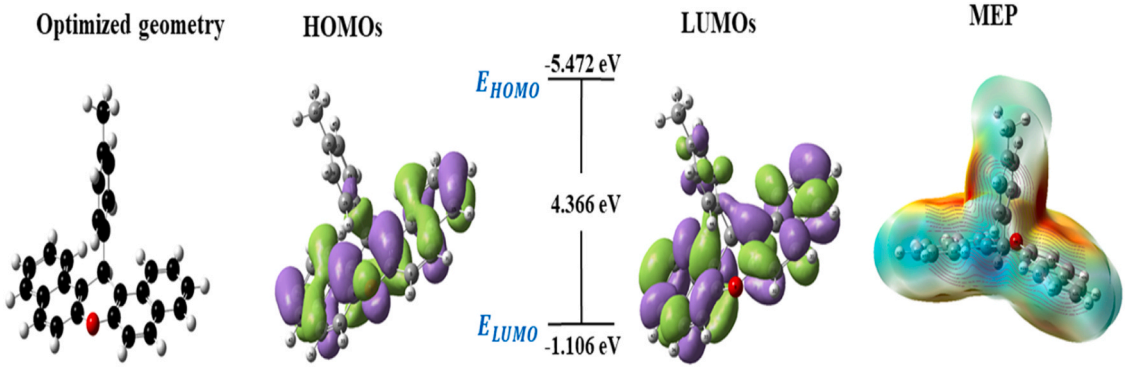

Fig. 11. Frontier Molecular Orbitals (FMO) of the ZM5 molecule and its Molecular Electrostatic Potential (MEP).

Table 7
Quantum chemical parameters calculated for the ZM5 inhibitor in gas and aqueous phases.

	Neutral								
B3LYP	E_{HOMO}	E_{LUMO}	ΔE_{gap}	χ	η	σ	ω	ε	Energy
Gas	−5.472	−1.106	4.366	3.289	2.183	0.4581	2.478	0.4036	−1154.315
Aqueous	−5.665	−1.289	4.376	3.477	2.188	0.457	2.763	0.362	−1154.324

Table 8
Computed values for ΔE_{b-d}, ΔN, $\Delta\psi$ and dipole moment (DM) for the ZM5 compound analyzed in both gas and aqueous phases.

Gas phase				Aqueous phase			
ΔN_{110}	$\Delta\psi$	$\Delta E_{b\text{-}d}$	μ (Debye)	ΔN_{110}	$\Delta\psi$	$\Delta E_{b\text{-}d}$	μ (Debye)
0.3507	−0.2684	−0.5458	0.698	0.3069	−0.2061	−0.547	1.047184

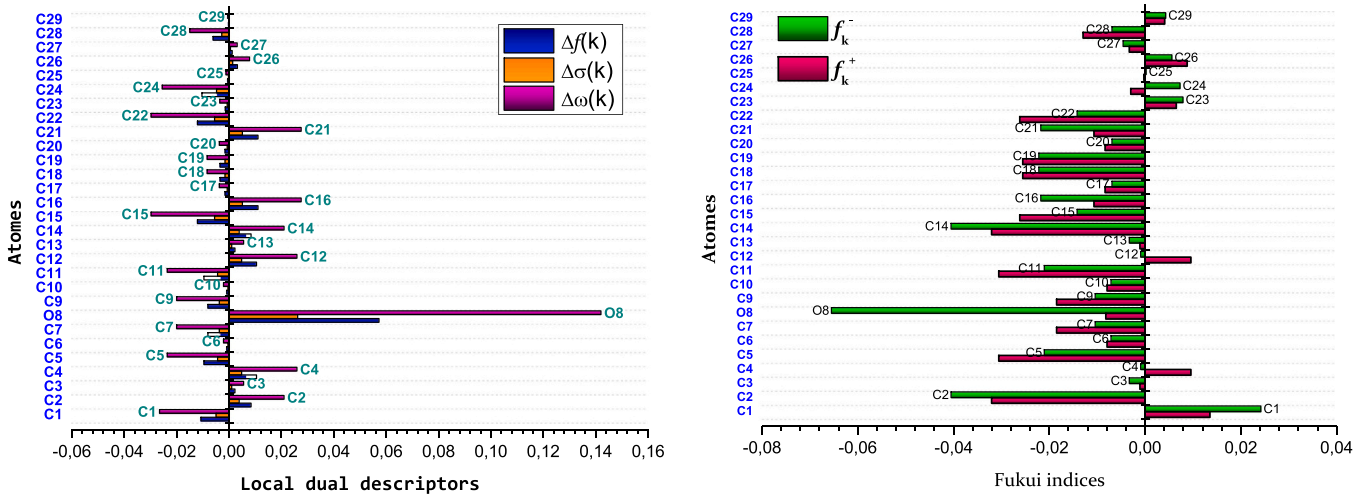

Fig. 12. Graphical representation of local dual descriptors $(\Delta f_k, \Delta\sigma and \Delta\omega)$ derived from fukui functions $\left(f_k^+, \quad f_k^-\right)$ for the ZM5 inhibitor.

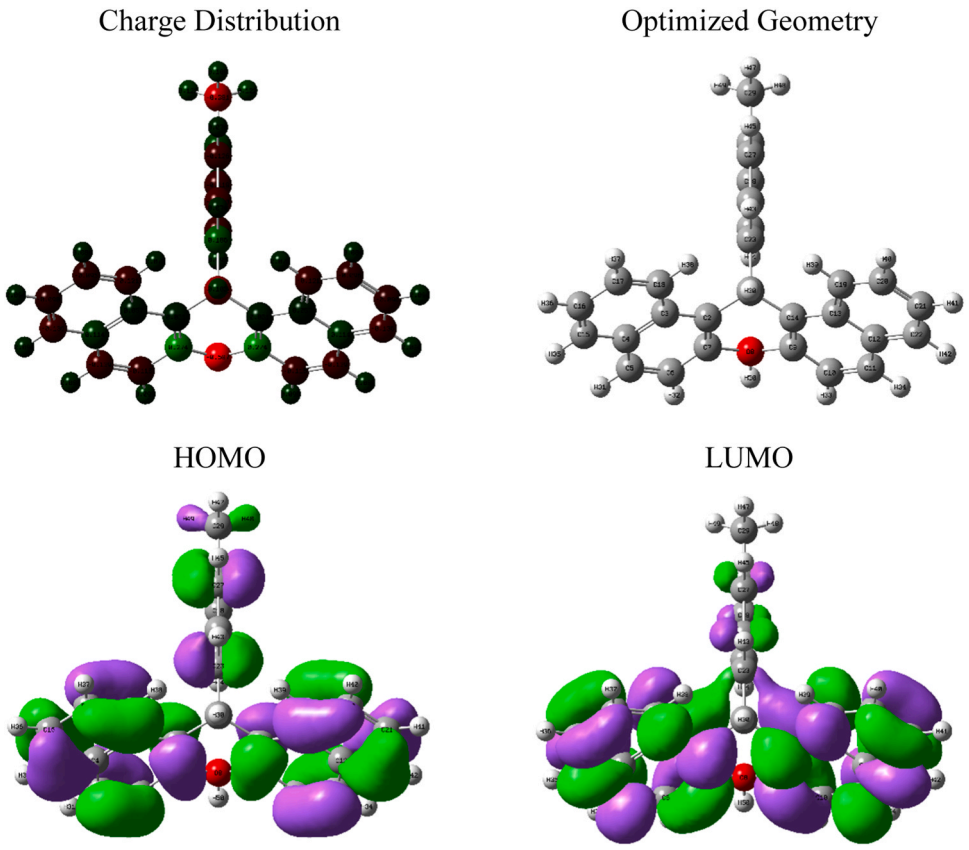

Fig. 13. Optimized geometry, charge distribution, and frontier molecular orbitals (HOMO and LUMO) of the studied inhibitor.

values for back-donation energy (ΔE_{b-d}), electron transfer fraction (ΔN), initial molecule-metal interaction energy (Δψ), and dipole moment (DM) reveal how ZM5 interacts with the metal surface, helping to evaluate its stability and effectiveness in preventing corrosion. By comparing these parameters across both phases, we can assess ZM5's adaptability and efficiency in different environmental conditions,

providing a deeper understanding of its molecular behavior as a corrosion inhibitor.

The ZM5 compound emerges as a highly promising corrosion inhibitor, demonstrating robust performance in both gas and aqueous environments. The key to its effectiveness lies in its ability to donate electrons, as reflected in the number of electrons transferred (ΔN 110). In the gas phase, ZM5 excels, with a higher electron transfer rate (0.3507), signaling its capacity to form a strong protective barrier on metal surfaces [90,91]. This heightened electron donation enhances its adsorption, making it a powerful shield against corrosion. The interaction energy (Δψ) supports this, with a more negative value in the gas phase (-0.2684 eV), further highlighting the strong bond formation between ZM5 and the metal surface, ensuring durable protection. What makes ZM5 even more compelling is its performance in aqueous environments, where corrosion is often more severe. Here, ZM5's dipole moment shines, increasing significantly to 1.047 Debye, a testament to its heightened polarity and improved interaction with water molecules. This increased polarity suggests that ZM5 can better anchor itself to metal surfaces in polar environments, enhancing its protective layer even in the face of aggressive aqueous corrosion. Despite these environmental differences, ZM5 remains consistently stable, as evidenced by the nearly identical back-donation energy values in both phases. This stability ensures that ZM5 can accept electrons from the metal surface, reinforcing its role as a versatile inhibitor that adapts to different conditions [92]. Whether in the gas phase with its superior electron-donating ability or in the aqueous phase with its enhanced polarity, ZM5 demonstrates a remarkable balance of properties, making it a top-tier candidate for comprehensive corrosion protection.

3.5.2. Fukui Functions

The Fukui function analysis provides valuable insights into the reactivity of different atoms within the studied molecule, particularly in terms of their susceptibility to nucleophilic, electrophilic, and radical attacks [93].

The Fukui function analysis of the ZM5 molecule reveals key reactive centers for nucleophilic, electrophilic, and radical attacks. Atoms like C1 and C26 are prone to nucleophilic attack, acting as electron acceptors, while C2 and C14 are more susceptible to electrophilic attack, donating electron density. The radical attack susceptibility highlights C1 and C23 as potential sites for radical formation or stabilization [93,94]. Oxygen atom O8, due to its high electronegativity, shows resistance to electrophilic attack but moderate involvement in nucleophilic and radical interactions. Overall, the molecule displays a well-distributed reactivity profile, allowing it to participate in a variety of chemical reactions depending on conditions.

The ZM5 inhibitor is a promising corrosion inhibitor that demonstrates significant potential in protecting metal surfaces from corrosive environments. By leveraging its molecular structure and quantum chemical properties, ZM5 interacts strongly with metal surfaces, forming a protective barrier that inhibits corrosion. The molecule's effectiveness is evident through its HOMO-LUMO energy gap, which indicates a balance between its electron-donating and electron-accepting abilities. Key atomic sites within ZM5, particularly oxygen O8, play a crucial role in its reactivity, as demonstrated by its high values in local dual descriptors such as Δf_k (nucleophilic reactivity), $\Delta\sigma$ (electrophilic reactivity), and $\Delta\omega$ (overall softness). These values highlight ZM5's capacity to interact with metal surfaces both as an electron donor and acceptor, facilitating the adsorption process that is essential for corrosion inhibition. In aqueous environments, ZM5's dipole moment further enhances its performance, allowing it to form stronger interactions in polar conditions. Overall, ZM5's balanced reactivity, high softness, and strong adsorption capabilities make it an effective and versatile inhibitor, particularly suited for applications where corrosion resistance is critical [94].

3.5.3. Protonated form of ZM5 molecule

To identify the reactive sites and determine the protonated form of the ZM5 compound, we utilized the Fukui indices calculated in the neutral state phase, along with the molecule's charge distribution. The Fukui indices, which indicate the likelihood of electron gain or loss at specific atomic sites, allow us to pinpoint regions most susceptible to protonation. By analyzing these indices in combination with the charge distribution, we can effectively identify the optimal protonation sites on the ZM5 molecule, thereby determining its most stable protonated form [94].

The oxygen atom O8, characterized by high electronegativity, effectively resists electrophilic attacks, thus limiting its role as an electron density donor in these interactions. However, this oxygen shows moderate participation in nucleophilic and radical interactions, thereby broadening the molecule's potential reaction spectrum. This ability of atom O8 to selectively participate in certain types of attacks contributes to the balanced reactivity profile of the ZM5 molecule.

3.6. Mechanism of the adsorption

The mechanism by which a corrosion inhibitor acts on a metal surface in an acidic environment can be influenced by the inhibitor's chemical structure, as well as by the nature and charge of the metal. The presence of heteroatoms and functional groups enhances the reactivity of the inhibitory molecule, thereby promoting the formation of a protective film on the metal. In our case, the inhibitor used is an organic compound, ZM5, which contains a heteroatom, oxygen. This oxygen atom imparts high reactivity to the ZM5 molecule, facilitating interaction with the metal surface and contributing to the formation of an effective protective film against corrosion in an acidic medium. Fig. 14 illustrates the schematic representation of the adsorption of the ZM5 molecule on the iron surface, based on results from experimental and theoretical studies.

4. Conclusion

This study highlights the remarkable corrosion inhibition properties of ZM5 for mild steel in a 1 M HCl solution, as evidenced by potentiodynamic polarization (PDP), electrochemical impedance spectroscopy (EIS), and adsorption analysis. PDP results indicate that ZM5 significantly suppresses both anodic and cathodic current densities, confirming its function as a mixed-type inhibitor. The high inhibition efficiencies (η_{PP}), reaching up to 94.7 %, reflect ZM5's capability to effectively mitigate corrosion rates by adsorbing its electron-rich heteroatoms onto the steel surface, forming a robust protective barrier. EIS data further validate the development of this protective layer,

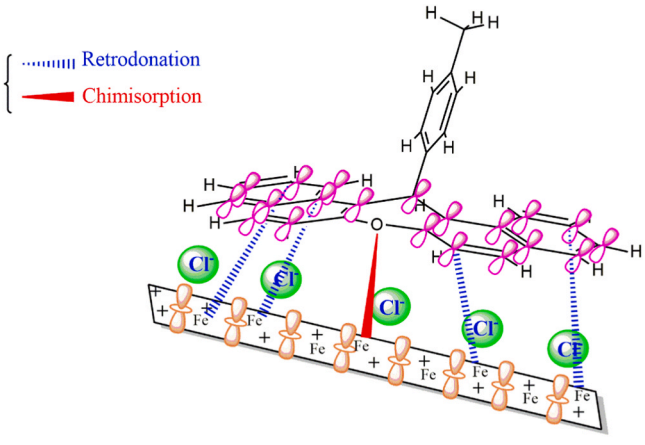

Fig. 14. Schematic representation of the adsorption mechanism of the ZM5 compound on the iron surface.

demonstrated by the rise in charge transfer resistance (R_{ct}) and the reduction in double-layer capacitance (C_{dl}) with increasing ZM5 concentration. Temperature studies reveal that ZM5 maintains its inhibitory effectiveness even at elevated temperatures, although a slight decline suggests a predominant physical adsorption mechanism. Langmuir isotherm analysis confirms chemical adsorption, indicating a strong interaction between ZM5 and the steel surface. Overall, ZM5 shows significant promise as a highly effective corrosion inhibitor for mild steel, offering durable protection through strong surface adsorption and stable inhibitor-metal complex formation. Density Functional Theory (DFT) calculations of descriptors further reinforce the observed trend in corrosion inhibition efficiency, emphasizing the role of ZM5.

CRediT authorship contribution statement

Said Boukhris: Formal analysis, Data curation. **Rafa Almeer:** Resources, Project administration. **Zakaria Benzekri:** Formal analysis, Conceptualization. **khadija Dahmani:** Writing – original draft. **Mohamed khattabi:** Methodology, Formal analysis. **Basheer M. Al-Maswari:** Supervision, Software. **Mohamed Ebn Touhami:** Validation, Supervision. **Azzeddine Belkheiri:** Writing – review & editing, Writing – original draft. **mouhsine galai:** Validation, Supervision. **Nadia Dkhireche:** Validation. **Khaoula Mzioud:** Writing – review & editing. **Otmane Kharbouch:** Software, Formal analysis.

Declaration of Competing Interest

The authors declare that they have no known competing financial interests or personal relationships that could have appeared to influence the work reported in this paper.

Acknowledgments

The authors would like to extend their sincere appreciation to the Researchers Supporting Project number (RSP2024R96), King Saud University, Riyadh, Saudi Arabia

References

[1] M.T. Muhammad, M.H. Hussin, M.H. Abu Bakar, T.S. Hamidon, S.S. Azahar, K. Awang, M. Litaudon, M.N. Azmi, Corrosion inhibitive performance of *Kopsia teoi* extracts towards mild steel in 0.5 M HCl solution, Mater. Chem. Phys. 322 (2024) 129584, https://doi.org/10.1016/j.matchemphys.2024.129584.

[2] H.M. Abd El-Lateef, A.O. Alnajjar, M.M. Khalaf, Advanced self-healing coatings based on ZnO, TiO2, and ZnO-TiO2/polyvinyl chloride nanocomposite systems for corrosion protection of carbon steel in acidic solutions containing chloride, J. Taiwan Inst. Chem. Eng. 116 (2020) 286–302, https://doi.org/10.1016/j.jtice.2020.11.015.

[3] D. de la Fuente, I. Díaz, J. Simancas, B. Chico, M. Morcillo, Long-term atmospheric corrosion of mild steel, Corros. Sci. 53 (2011) 604–617, https://doi.org/10.1016/j.corsci.2010.10.007.

[4] M.A. Hegazy, A.S. El-Tabei, A.H. Bedair, M.A. Sadeq, Synthesis and inhibitive performance of novel cationic and gemini surfactants on carbon steel corrosion in 0.5 M H2SO4 solution, RSC Adv. 5 (2015) 64633–64650, https://doi.org/10.1039/C5RA06473B.

[5] Z. Fang, S. Fu, Y. Peng, X. Yang, Q. Sun, P. Li, H. Ma, R. Zhang, Z. Liang, J. Li, Developing a novel imine derivative as a corrosion inhibitor for Q235 carbon steel in 1 M HCl solution: experiments and theoretical calculations, Mater. Today Commun. 40 (2024) 109693, https://doi.org/10.1016/j.mtcomm.2024.109693.

[6] A. Guendouz, W. Ettahiri, M. Adardour, J. Lazrak, E.H.E. Assiri, A. Taleb, B. Hammouti, Z. Rais, A. Baouid, M. Taleb, New benzimidazole derivatives as efficient organic inhibitors of mild steel corrosion in hydrochloric acid medium: electrochemical, SEM/EDX, MC, and DFT studies, J. Mol. Struct. (2024) 139901, https://doi.org/10.1016/j.molstruc.2024.139901.

[7] A. Toghan, H. Alhussain, A. Fawzy, M.M.S. Sanad, S.A. Al-Hussain, E.M. Masoud, H. Jiang, A.A. Farag, One-pot synthesis of N'-(thiophen-2-ylmethylene) isonicotinohydrazide Schiff-base as a corrosion inhibitor for C-steel in 1 M HCl: theoretical, electrochemical, adsorption and spectroscopic inspections, J. Mol. Struct. 1318 (2024) 139315, https://doi.org/10.1016/j.molstruc.2024.139315.

[8] N. Dkhireche, M. Galai, Y. El Kacimi, M. Rbaa, M. Ouakki, B. Lakhrissi, M. E. Touhami, New quinoline derivatives as sulfuric acid inhibitor's for mild steel, Anal. Bioanal. Electrochem 10 (2018) 111–135.

[9] K. Mzioud, A. Habsaoui, S. Rached, R. Lachhab, N. Dkhireche, M. Ouakki, M. Galai, E. Souad, M. Touhami, Synergistic Effect from Allium sativum Essential Oil and Diethylthiourea for Corrosion Inhibition of Carbon Steel in 0.5 M H2SO4 Medium, in: 2022: pp. 251–266. https://doi.org/10.1007/978-3-031-11397-0_23.

[10] A.K. Sheetal, V.C. Singh, M. Anadebe, N. Singh, R.C. Arshad, M.A.U.R. Barik, T. W. Qureshi, E.D. Quadri, L.O. Akpan, S.K. Olasunkanmi, J. Shukla, S. Tuteja, B. Thakur, E.E. Pani, Ebenso, Coordination chemistry of chalcones and derivatives and their use as corrosion inhibitors: a comprehensive review, Coord. Chem. Rev. 517 (2024) 215985, https://doi.org/10.1016/j.ccr.2024.215985.

[11] R. Bender, D. Féron, D. Mills, S. Ritter, R. Bäßler, D. Bettge, I. De Graeve, A. Dugstad, S. Grassini, T. Hack, M. Halama, E.-H. Han, T. Harder, G. Hinds, J. Kittel, R. Krieg, C. Leygraf, L. Martinelli, A. Mol, D. Neff, J.-O. Nilsson, I. Odnevall, S. Paterson, S. Paul, T. Prošek, M. Raupach, R.I. Revilla, F. Ropital, H. Schweigart, E. Szala, H. Terryn, J. Tidblad, S. Virtanen, P. Volovitch, D. Watkinson, M. Wilms, G. Winning, M. Zheludkevich, Corrosion challenges towards a sustainable society, Mater. Corros. 73 (2022) 1730–1751, https://doi.org/10.1002/maco.202213140.

[12] S. Km, B.M. Praveen, B.K. Devendra, A review on corrosion inhibitors: types, mechanisms, electrochemical analysis, corrosion rate and efficiency of corrosion inhibitors on mild steel in an acidic environment, Results Surf. Interfaces 16 (2024) 100258, https://doi.org/10.1016/j.rsurfi.2024.100258.

[13] W. Hua, X. Xu, X. Zhang, H. Yan, J. Zhang, Progress in corrosion and anti-corrosion measures of phase change materials in thermal storage and management systems, J. Energy Storage 56 (2022) 105883, https://doi.org/10.1016/j.est.2022.105883.

[14] Y. He, X. Qi, Z. Peng, Y. Ren, H. Yang, X. Liu, Green inhibitor loaded functional halloysite nanotubes modified coatings for improving corrosion protection of carbon steel, Mater. Today Commun. 38 (2024) 108231, https://doi.org/10.1016/j.mtcomm.2024.108231.

[15] P. Zarras, J.D. Stenger-Smith, 1 - Corrosion processes and strategies for prevention: an introduction, in: A.S.H. Makhlouf (Ed.), Handb. Smart Coat. Mater. Prot., Woodhead Publishing, 2014, pp. 3–28, https://doi.org/10.1533/9780857096883.1.3.

[16] Y. Zhang, Y. Qin, Y. Sun, X. Liu, Z. Wang, Synthesis, characterization and anticorrosion performance of a new corrosion inhibitor based on cobalt-phenanthroline- p-hydroxybenzoic acid ternary complex, Mater. Today Commun. 41 (2024) 110362, https://doi.org/10.1016/j.mtcomm.2024.110362.

[17] N. Ferraa, M. Ouakki, M. Cherkaoui, M. Ziatni, Study of the Inhibitory Action of Apatitic Tricalcium Phosphate on Carbon Steel in Two Acidic Media (HCl 1.0 M and H2SO4 0.5 M), in: 2022: pp. 159–176. https://doi.org/10.1007/978-3-031-11397-0_14.

[18] N. Ferraa, M. Ouakki, M. Cherkaoui, M. Bennani-Ziatni, Synthesis, characterization and evaluation of apatitic tricalcium phosphate as a corrosion inhibitor for carbon steel in 3 wt% NaCl, J. Bio- Tribo-Corros. 8 (2022), https://doi.org/10.1007/s40735-021-00622-4.

[19] N. Ferraa, M. Ouakki, H. El Harmouchi, M. Cherkaoui, M. Bennani Ziatni, Investigation of the inhibition behavior of an octacalcium phosphate as a green corrosion inhibitor against carbon steel in 3% NaCl medium, Inorg. Chem. Commun. 157 (2023), https://doi.org/10.1016/j.inoche.2023.111343.

[20] A. Belkheiri, K. Dahmani, K. Mzioud, M. Rbaa, M. Galai, A. Hmada, B. Erdoğan, M. E. Tüzün, H.A. Touhami, B.M. El-Serehy, Al-Maswari, Advanced evaluation of novel quinoline derivatives for corrosion inhibition of mild steel in acidic environments: a comprehensive electrochemical, computational, and surface study, Int. J. Electrochem. Sci. 19 (2024) 100772, https://doi.org/10.1016/j.ijoes.2024.100772.

[21] K. Mzioud, A. Habsaoui, S. Rached, E. Ech-chihbi, M. Ouakki, R. Salghi, M. E. Touhami, Experimental investigation and theoretical modeling of copper corrosion inhibition by *Urginea maritima* essential oil, Mater. Today Sustain. (2024) 100906, https://doi.org/10.1016/j.mtsust.2024.100906.

[22] S. Rached, K. Mzioud, A. Habsaoui, M. Galai, K. Dahmani, M. Ouakki, S. El Fartah, N. Dkhireche, M. Ebn Touhami, Inhibition of copper corrosion in sulfuric acid by mentha pulegium L. Port. Electrochim. Acta 42 (2024) 137–153, https://doi.org/10.4152/pea.2023420205.

[23] S. Rached, A. Habsaoui, K. Mzioud, R. Lachhab, S. Haida, N. Errahmany, M. Galai, M.E. Touhami, Valorization of the green corrosion inhibitor marrubium vulgare L.: electrochemical, thermodynamic, theoretical & surface studies, Chem. Data Collect. 48 (2023), https://doi.org/10.1016/j.cdc.2023.101099.

[24] S. Rached, H. Imatara, A. Habsaoui, K. Mzioud, S. Haida, A. Saleh, O. Al kamaly, A. Alahdab, M.K. Parvez, S. Ourras, S. El Fartah, Characterization, chemical compounds and biological activities of marrubium vulgare L. essential oil, Processes 10 (2022) 2110, https://doi.org/10.3390/pr10102110.

[25] G. Doumane, J. Bensalah, M. Ouakki, Z. Aribou, O. Boussalem, K. Mzioud, Z.S. Safi, A. Berisha, M. Bourhia, A.-R. Z. Gaafar, S. Ibenmoussa, G.F. Wondmie, A. Zarrouk, M.E. Touhami, A. Habsaoui, Alkaloid extract of seed Citrullus colocynthis as novel green inhibitor for mild steel corrosion in one molar HCl acid solution: DFT and MC/MD approaches, Sci. Rep. 14 (2024) 16857, https://doi.org/10.1038/s41598-024-67011-y.

[26] K. Mzioud, A. Habsaoui, H. Imatra, S. Haida, S. Rached, S. Msairi, A. Douira, A. S. Alqahtani, O.M. Noman, M. Tarayrah, M.E. Touhami, Physicochemical characterization, antioxidant and antifungal activities of essential oils of Urginea maritima and Allium sativum, Open Chem. 21 (2023), https://doi.org/10.1515/chem-2023-0149.

[27] M. Ouakki, M. Galai, Z. Aribou, M. Rbaa, B. Lakhrissi, M. Cherkaoui, Novel compounds of imidazole derivatives as effective corrosion inhibitors for mild steel in hydrochloric acid solution, Electrochem. Spectrosc. Charact., (2020) 132–155, https://doi.org/10.4018/978-1-7998-2775-7.ch006.

[28] Z. Aribou, M. Ouakki, N. Khemmou, S. Sibous, E. Ech-chihbi, Z. Benzekri, M. Galai, S. Boukhris, A.A. AlObaid, I. Warad, M.E. Touhami, Detailed experimental of indazole derivatives as corrosion inhibitor for brass in acidic environment:

electrochemical/theoretical/surface studies, J. Appl. Electrochem. 54 (2024) 393–411, https://doi.org/10.1007/s10800-023-01960-6.
[29] Z. Aribou, M. Ouakki, N. Khemmou, S. Sibous, E. Ech-chihbi, O. Kharbouch, M. Galai, A. Souizi, S. Boukhris, M.E. Touhami, A.A. AlObaid, I. Warad, Exploring the adsorption and corrosion inhibition properties of indazole as a corrosion inhibitor for brass alloy in HCl medium: a theoretical and experimental study, Mater. Today Commun. 37 (2023), https://doi.org/10.1016/j.mtcomm.2023.107061.
[30] Z. Aribou, N. Khemmou, R. Allah Belakhmima, I. Chaouki, M. Ebn Touhami, R. Touir, S. Bakkali, Effect of polymer additive on structural and morphological properties of Cu-electrodeposition from an acid sulfate electrolyte: experimental and theoretical studies, J. Electroanal. Chem. 946 (2023), https://doi.org/10.1016/j.jelechem.2023.117722.
[31] A. Belkheiri, K. Dahmani, Z. Aribou, O. Kharbouch, E. Nordine, A.E. Moutaouakil Ala Allah, M. Galai, M.E. Touhami, M.K. Al-Sadoon, B.M. Al-Maswari, Y. Ramli, In-depth study of a newly synthesized imidazole derivative as an eco-friendly corrosion inhibitor for mild steel in 1 M HCl: theoretical, electrochemical, and surface analysis perspectives, Int. J. Electrochem. Sci. 19 (2024), https://doi.org/10.1016/j.ijoes.2024.100768.
[32] N. Timoudan, A.S. Al-Gorair, L.E. Foujji, I. Warad, Z. Safi, B. Dikici, F. Benhiba, A. E.K. Qaiss, R. Bouhfid, F. Bentiss, S.S. Al-Juaid, M. Abdallah, A. Zarrouk, Corrosion inhibition performance of benzimidazole derivatives for protection of carbon steel in hydrochloric acid solution, RSC Adv. 14 (2024) 30295–30316, https://doi.org/10.1039/D4RA05070C.
[33] M.G.A. Saleh, M. Alfakeer, R.N. Felaly, M.S. Al-Sharif, S.S. Al-Juaid, K.A. Soliman, M.A. Hegazy, S. Nooh, M. Abdallah, S.A. El Wanees, Retardation of the C-steel destruction in hydrochloric acid media utilizing an effective schiff base inhibitor: experimental and theoretical computations, ACS Omega 9 (2024) 29666–29681, https://doi.org/10.1021/acsomega.4c03135.
[34] M. Abdallah, K.A. Soliman, M. Alfakeer, A.M. Al-bonayan, M.T. Alotaibi, H. Hawsawi, O.A. Hazazi, R.S. Abdel Hameed, M. Sobhi, Mitigation effect of natural lettuce oil on the corrosion of mild steel in sulfuric acid solution: chemical, electrochemical, computational aspects, Green. Chem. Lett. Rev. 16 (2023) 2249019, https://doi.org/10.1080/17518253.2023.2249019.
[35] M. Abdallah, T. Al-Habal, R. El-Sayed, M.I. Awad, R.S.A. Hameed, Corrosion control of carbon steel in acidic media by nonionic surfactant compounds derived from 1,3,4-oxadiazole and 1,3,4-thiadiazole, Int. J. Electrochem. Sci. 17 (2022) 221255, https://doi.org/10.20964/2022.12.63.
[36] H.B. Mahood, A. Sayer, A. Mekky, A. Khadom, Performance of synthesized acetone based inhibitor on low carbon steel corrosion in 1 M HCL solution, Chem. Afr. 3 (2019), https://doi.org/10.1007/s42250-019-00104-8.
[37] A.A. Fadhil, A.A. Khadom, H. Liu, C. Fu, J. Wang, N.A. Fadhil, H.B. Mahood, *S)-6-Phenyl-2,3,5,6-tetrahydroimidazo[2,1-b] thiazole* hydrochloride as corrosion inhibitor of steel in acidic solution: gravimetrical, electrochemical, surface morphology and theoretical simulation, J. Mol. Liq. 276 (2019) 503–518, https://doi.org/10.1016/j.molliq.2018.12.015.
[38] S.K. Ahmed, W.B. Ali, A.A. Khadom, Synthesis and characterization of new triazole derivatives as corrosion inhibitors of carbon steel in acidic medium, J. Bio- Tribo-Corros. 5 (2018) 15, https://doi.org/10.1007/s40735-018-0209-1.
[39] S.K. Ahmed, W.B. Ali, A.A. Khadom, Synthesis and investigations of heterocyclic compounds as corrosion inhibitors for mild steel in hydrochloric acid, Int. J. Ind. Chem. 10 (2019) 159–173, https://doi.org/10.1007/s40090-019-0181-8.
[40] B.E.A. Rani, B.B.J. Basu, Green inhibitors for corrosion protection of metals and alloys: an overview, Int. J. Corros. (2011) (2012) e380217, https://doi.org/10.1155/2012/380217.
[41] Y. El aoufir, S. Zehra, H. Lgaz, A. Chaouiki, H. Serrar, S. Kaya, R. Salghi, S. K. AbdelRaheem, S. Boukhris, A. Guenbour, I.-M. Chung, Evaluation of inhibitive and adsorption behavior of thiazole-4-carboxylates on mild steel corrosion in HCl, Colloids Surf. Physicochem. Eng. Asp. 606 (2020) 125351, https://doi.org/10.1016/j.colsurfa.2020.125351.
[42] I.B. Onyeachu, M.M. Solomon, Benzotriazole derivative as an effective corrosion inhibitor for low carbon steel in 1 M HCl and 1 M HCl + 3.5 wt% NaCl solutions, J. Mol. Liq. 313 (2020) 113536, https://doi.org/10.1016/j.molliq.2020.113536.
[43] E.E. Ebenso, Effect of halide ions on the corrosion inhibition of mild steel in H2SO4 using methyl red: Part 1, Bull. Electrochem. 19 (2003) 209–216.
[44] J. Tang, Y. Shi, S. He, J. Luo, Y. Liu, K. Zhai, M. Duan, H. Wang, J. Xie, Study on the corrosion inhibition properties of some quinoline derivatives as acidizing corrosion inhibitors for steel, Int. J. Electrochem. Sci. 19 (2024) 100547, https://doi.org/10.1016/j.ijoes.2024.100547.
[45] V.V. Torres, V.A. Rayol, M. Magalhães, G.M. Viana, L.C.S. Aguiar, S.P. Machado, H. Orofino, E. D'Elia, Study of thioureas derivatives synthesized from a green route as corrosion inhibitors for mild steel in HCl solution, Corros. Sci. 79 (2014) 108–118, https://doi.org/10.1016/j.corsci.2013.10.032.
[46] L. Fan, P. Wang, Y. Song, K.R. Ansari, H. Li, A. Singh, X. Kong, Y. Lin, M. Talha, Two schiff base as corrosion inhibitors for N80 in 1.0 M HCl: experimental and theoretical studies, J. Indian Chem. Soc. 101 (2024) 101316, https://doi.org/10.1016/j.jics.2024.101316.
[47] L.R. Chauhan, G. Gunasekaran, Corrosion inhibition of mild steel by plant extract in dilute HCl medium, Corros. Sci. 49 (2007) 1143–1161.
[48] Y. Merroun, S. Chehab, A. El Hallaoui, T. Guedira, S. Boukhris, R. Ghailane, A. Souizi, Triple superphosphate modified by tin (II) chloride: as a reusable and efficient catalyst for the one-pot synthesis of xanthene and xanthenone derivatives under green conditions, J. Mol. Struct. 1294 (2023) 136383.
[49] S.R. Tokgöz, Y.E. Firat, Z. Safi, A. Peksoz, Electrochemical properties of Al doped polypyrrole composite polymer: mott-schottky approximation and density functional theory, J. Electrochem. Soc. 166 (2019) G54.
[50] N.A. Odewunmi, M.A.J. Mazumder, S.A. Ali, B.G. Alharbi, Hydroquinone decorated with alkyne, quaternary ammonium, and hydrophobic motifs to mitigate corrosion of X-60 Mild Steel in 15 wt% HCl, Chem. Asian J 16 (2021) 801–821, https://doi.org/10.1002/asia.202100085. Hydroquinone decorated with alkyne, quaternary ammonium, and hydrophobic motifs to mitigate corrosion of X-60 Mild Steel in 15wt% HCl, Chem. - Asian J.
[51] L. Guo, Z.S. Safi, S. Kaya, W. Shi, B. Tüzün, N. Altunay, C. Kaya, Anticorrosive effects of some thiophene derivatives against the corrosion of iron: a computational study, Front. Chem. 6 (2018), https://doi.org/10.3389/fchem.2018.00155.
[52] Y. Lakhrissi, M. Rbaa, B. Tuzun, A. Hichar, E.H. Anouar, K. Ounine, F. Almalki, T. Ben Hadda, A. Zarrouk, B. Lakhrissi, Synthesis, structural confirmation, antibacterial properties and bio-informatics computational analyses of new pyrrole based on 8-hydroxyquinoline, J. Mol. Struct. 1259 (2022), https://doi.org/10.1016/j.molstruc.2022.132683.
[53] Z. El Adnani, M. Mcharfi, M. Sfaira, M. Benzakour, A.T. Benjelloun, M. Ebn Touhami, DFT theoretical study of 7-R-3methylquinoxalin-2(1H)-thiones (RH; CH3; Cl) as corrosion inhibitors in hydrochloric acid, Corros. Sci. 68 (2013) 223–230, https://doi.org/10.1016/j.corsci.2012.11.020.
[54] I.B. Obot, D.D. Macdonald, Z.M. Gasem, Density functional theory (DFT) as a powerful tool for designing new organic corrosion inhibitors: Part 1: an overview, Corros. Sci. 99 (2015) 1–30, https://doi.org/10.1016/j.corsci.2015.01.037.
[55] I.H. Ali, R. Marzouki, Y.Ben Smida, A. Brahmia, M.F. Zid, Inhibition effect of Coleus forskohlii leaf extract on Steel Corrosion in 1.0 M HCl solution: experimental and theoretical approaches, Int. J. Electrochem. Sci. 13 (2018) 11580–11595, https://doi.org/10.20964/2018.12.53.
[56] K. Abderrahim, O.M.A. Khamaysa, I. Selatnia, H. Zeghache, Adsorption and performance assessment of 5-Mercapto-1-Methyl Tetrazole as A9M steel corrosion inhibitor in HCl medium: A detailed experimental, and computational methods, Chem. Data Collect. 39 (2022) 100848.
[57] K. Abderrahim, O.M.A. Khamaysa, I. Selatnia, H. Zeghache, Adsorption and performance assessment of 5-Mercapto-1-Methyl Tetrazole as A9M steel corrosion inhibitor in HCl medium: a detailed experimental, and computational methods, Chem. Data Collect. 39 (2022), https://doi.org/10.1016/j.cdc.2022.100848.
[58] N.B. Iroha, N.A. Madueke, V. Mkpenie, B.T. Ogunyemi, L.A. Nnanna, S. Singh, E. D. Akpan, E.E. Ebenso, Experimental, adsorption, quantum chemical and molecular dynamics simulation studies on the corrosion inhibition performance of Vincamine on J55 steel in acidic medium, J. Mol. Struct. 1227 (2021), https://doi.org/10.1016/j.molstruc.2020.129533.
[59] K. Rasheeda, A.H. Alamri, P.A. Krishnaprasad, N.P. Swathi, V.D.P. Alva, T. A. Aljohani, Efficiency of a pyrimidine derivative for the corrosion inhibition of C1018 carbon steel in aqueous acidic medium: experimental and theoretical approach, Colloids Surf. Physicochem. Eng. Asp. 642 (2022), https://doi.org/10.1016/j.colsurfa.2022.128631.
[60] Z. Aribou, M. Ouakki, F. El Hajri, E. Ech-chihbi, I. Saber, Z. Benzekri, S. Boukhris, M.K. Al-Sadoon, M. Galai, J. Charafeddine, M.E. Touhami, Comprehensive assessment of the corrosion inhibition properties of quinazoline derivatives on mild steel in 1.0 M HCl solution: an electrochemical, surface analysis, and computational study, Int. J. Electrochem. Sci. 19 (2024) 100788, https://doi.org/10.1016/j.ijoes.2024.100788.
[61] B. Tan, Z. Gong, W. He, J. Xiong, L. Guo, R. Marzouki, Insight into the anti-corrosion mechanism of crop waste Arachis hypogaea L. leaf extract for copper in sulfuric acid medium, Sustain. Chem. Pharm. 38 (2024), https://doi.org/10.1016/j.scp.2024.101449.
[62] A. Ech-chebab, M. Missioui, L. Guo, O. El Khouja, R. Lachhab, O. Kharbouch, M. Galai, M. Ouakki, A. Ejbouh, K. Dahmani, N. Dkhireche, M. Ebn Touhami, Evaluation of quinoxaline-2(1H)-one, derivatives as corrosion inhibitors for mild steel in 1.0 M acidic media: electrochemistry, quantum calculations, dynamic simulations, and surface analysis, Chem. Phys. Lett. 809 (2022) 140156, https://doi.org/10.1016/j.cplett.2022.140156.
[63] M.R. Rathod, R.L. Minagalavar, S.K. Rajappa, Effect of *Artabotrys odoratissimus* extract as an environmentally sustainable inhibitor for mild steel corrosion in 0.5 M H2SO4 media, J. Indian Chem. Soc. 99 (2022) 100445, https://doi.org/10.1016/j.jics.2022.100445.
[64] H. Kahkesh, B. Zargar, Estimating the anti-corrosive potency of 3-nitrophthalic acid as a novel and natural organic inhibitor on corrosion monitoring of mild steel in 1 M HCl solution, Inorg. Chem. Commun. 158 (2023) 111533, https://doi.org/10.1016/j.inoche.2023.111533.
[65] M.P. Asfia, M. Rezaei, G. Bahlakeh, Corrosion prevention of AISI 304 stainless steel in hydrochloric acid medium using garlic extract as a green corrosion inhibitor: electrochemical and theoretical studies, J. Mol. Liq. 315 (2020) 113679, https://doi.org/10.1016/j.molliq.2020.113679.
[66] S.K. Singh, S.P. Tambe, G. Gunasekaran, V.S. Raja, D. Kumar, Electrochemical impedance study of thermally sprayable polyethylene coatings, Corros. Sci. 51 (2009) 595–601, https://doi.org/10.1016/j.corsci.2008.11.025.
[67] J. Zhu, B. Lin, T. Duan, H. Lin, G. Zhang, X. Zhou, Y. Xu, *Zea mays* bracts extract as an eco-friendly corrosion inhibitor for steel in HCl pickling solution: experimental and simulation studies, Arab. J. Chem. 17 (2024) 105895, https://doi.org/10.1016/j.arabjc.2024.105895.
[68] F.S. de Souza, A. Spinelli, Caffeic acid as a green corrosion inhibitor for mild steel, Corros. Sci. 51 (2009) 642–649, https://doi.org/10.1016/j.corsci.2008.12.013.
[69] Z.V.P. Murthy, K. Vijayaragavan, Mild steel corrosion inhibition by acid extract of leaves of Hibiscus sabdariffa as a green corrosion inhibitor and sorption behavior, Green. Chem. Lett. Rev. 7 (2014) 209–219, https://doi.org/10.1080/17518253.2014.924592.

[70] M.A. Ameer, A.M. Fekry, Corrosion inhibition of mild steel by natural product compound, Prog. Org. Coat. 71 (2011) 343–349, https://doi.org/10.1016/j.porgcoat.2011.04.001.
[71] N.N. Hau, D.Q. Huong, Effect of aromatic rings on mild steel corrosion inhibition ability of nitrogen heteroatom-containing compounds: experimental and theoretical investigation, J. Mol. Struct. 1277 (2023) 134884, https://doi.org/10.1016/j.molstruc.2022.134884.
[72] I. El Ouali, A. Chetouani, B. Hammouti, A. Aouniti, R. Touzani, S. El Kadiri, S. Nlate, Thermodynamic study and characterization by electrochemical technique of pyrazole derivatives as corrosion inhibitors for C38 Steel in molar hydrochloric acid, Port. Electrochim. Acta 31 (2013) 53–78, https://doi.org/10.4152/pea.201302053.
[73] K. Tarfaoui, N. Brhadda, M. Ouakki, M. Galai, E. Ech-chihbi, K. Atfaoui, M. Khattabi, M. Nehiri, R. Lachhab, M. Ebn Touhami, M. Ouhssine, Natural elettaria cardamomum essential oil as a sustainable and a green corrosion inhibitor for mild steel in 1.0 M HCl solution: electrochemical and computational methods, J. Bio- Tribo-Corros. 7 (2021) 131, https://doi.org/10.1007/s40735-021-00567-8.
[74] M. Ouakki, M. Galai, M. Cherkaoui, E.-H. Rifi, Z. Hatim, Inorganic compound (Apatite doped by Mg and Na) as a corrosion inhibitor for mild steel in phosphoric acidic medium, Anal. Bioanal. Electrochem. 10 (2018) 943–960.
[75] S.A. Ali, A.M. El-Shareef, R.F. Al-Ghamdi, M.T. Saeed, The isoxazolidines: the effects of steric factor and hydrophobic chain length on the corrosion inhibition of mild steel in acidic medium, Corros. Sci. 47 (2005) 2659–2678, https://doi.org/10.1016/j.corsci.2004.11.007.
[76] A. Tazouti, N. Errahmany, M. Rbaa, M. Galai, Z. Rouifi, R. Touir, A. Zarrouk, S. Kaya, M.E. Touhami, B. El Ibrahimi, S. Erkan, Effect of hydrocarbon chain length for acid corrosion inhibition of mild steel by three 8-(n-bromo-R-alkoxy)quinoline derivatives: experimental and theoretical investigations, J. Mol. Struct. 1244 (2021) 130976, https://doi.org/10.1016/j.molstruc.2021.130976.
[77] H.E. Harmouchi, O. Moumouche, S. Alami, A. Hmada, R. Khaoulaf, K. Brouzi, M. E. Touhami, M. Harcharras, Vibrational Spectroscopy and electrochemical study of MCuP2O7 (M = Ba, Ca and Zn), improvement of corrosion resistance of mild steel in 1.0 M HCl medium, J. Mol. Struct. 1284 (2023) 135452, https://doi.org/10.1016/j.molstruc.2023.135452.
[78] R. Khrifou, R. Touir, A. Koulou, H.E. Bakri, M. Rbaa, M.E. Touhami, A. Zarrouk, F. Benhiba, The influence of low concentration of 2-(5-methyl-2-nitro-1H-imidazol-1-yl)ethyl benzoate on corrosion brass in 0.5 M H2SO4 solution, Surf. Interfaces 24 (2021), https://doi.org/10.1016/j.surfin.2021.101088.
[79] H. El Harmouchi, S. Alami, O. Moumouche, A. El Amri, M. Ouakki, K. Brouzi, R. Khaoulaf, N. Dkhireche, M. Harcharras, Synthesis of ZnSrP2O7 and CoSrP2O7 Pyrophosphates: characterization, vibrational properties and electrochemical performance on mild steel in an acidic environment, Inorg. Chem. Commun. 166 (2024) 112593, https://doi.org/10.1016/j.inoche.2024.112593.
[80] K. Dahmani, M. Galai, M. Rbaa, A. Ech-Chebab, N. Errahmany, L. Guo, A. A. AlObaid, A. Hmada, I. Warad, B. lakhrissi, M. Ebn Touhami, M. Cherkaoui, Evaluating the efficacy of synthesized quinoline derivatives as Corrosion inhibitors for mild steel in acidic environments: an analysis using electrochemical, computational, and surface techniques, J. Mol. Struct. 1295 (2024) 136514, https://doi.org/10.1016/j.molstruc.2023.136514.
[81] E. Li, J. Zhang, B. Wang, P. Yao, Combined electrochemical, surface analysis and DFT/MD-simulations to evaluate choline histidine ionic liquid as a green corrosion inhibitor for mild steel in neutral medium, Mater. Today Commun. 40 (2024) 109871, https://doi.org/10.1016/j.mtcomm.2024.109871.
[82] M.M.Y. Modwi, H. Feng, M.K. Hadi, N. Chen, J. Hou, E. Kamal, K. Yang, Eco-friendly corrosion inhibitor of Q235 carbon steel in 1.0 M HCl by Isatin/Chitosan Schiff base, J. Mol. Struct. 1321 (2025) 139592, https://doi.org/10.1016/j.molstruc.2024.139592.
[83] H. Deng, B. Li, H. Ren, C. Kang, X. Li, B. Tan, L. Guo, M.K. Al-Sadoon, Investigation of the corrosion inhibitory effectiveness of castor leaf extract as a corrosion inhibitor for steel in a sulfuric acid environment, J. Environ. Chem. Eng. 12 (2024) 113974, https://doi.org/10.1016/j.jece.2024.113974.
[84] M. Khattabi, F. Benhiba, S. Tabti, A. Djedouani, H. Zarrok, A. Boutakiout, R. Touzani, I. Warad, M.E. Touhami, H. Oudda, A. Zarrouk, The study of a new pyran compound in two distinct environments: 0.5 M H2SO4 And 1.0 M HCl As an inhibitor and combines experimental evaluations with computational analytics to assess its performance, Anal. Bioanal. Electrochem. 15 (2023) 739–766, https://doi.org/10.22034/abec.2023.708105.
[85] M. Özcan, I. Dehri, M. Erbil, Organic sulphur-containing compounds as corrosion inhibitors for mild steel in acidic media: correlation between inhibition efficiency and chemical structure, Appl. Surf. Sci. 236 (2004) 155–164, https://doi.org/10.1016/j.apsusc.2004.04.017.
[86] J. Frau, D. Glossman-Mitnik, Conceptual dft descriptors of amino acids with potential corrosion inhibition properties calculated with the latest minnesota density functionals, Front. Chem. 5 (2017) 1–8, https://doi.org/10.3389/fchem.2017.00016.
[87] L. Guo, Y.El Bakri, R. Yu, J. Tan, E.M. Essassi, Newly synthesized triazolopyrimidine derivative as an inhibitor for mild steel corrosion in hcl medium: an experimental and in silico study, J. Mater. Res. Technol. 9 (2020) 6568–6578, https://doi.org/10.1016/j.jmrt.2020.04.044.
[88] R. Hsissou, S. Abbout, Z. Safi, F. Benhiba, N. Wazzan, L. Guo, K. Nouneh, S. Briche, H. Erramli, M. Ebn Touhami, M. Assouag, A. Elharfi, Synthesis and anticorrosive properties of epoxy polymer for CS in [1 M] HCl solution: ELectrochemical, AFM, DFT and MD simulations, Constr. Build. Mater. 270 (2021), https://doi.org/10.1016/j.conbuildmat.2020.121454.
[89] A. Ech-chebab, M. Missioui, L. Guo, O. El, R. Lachhab, Evaluation of quinoxaline-2 (1H) -one, derivatives as corrosion inhibitors for mild steel in 1. 0 M acidic media: electrochemistry, quantum calculations, Dyn. Simul., Surf. Anal. 809 (2022).
[90] S. Gurjar, S.K. Sharma, A. Sharma, S. Ratnani, Performance of imidazolium based ionic liquids as corrosion inhibitors in acidic medium: a review, Appl. Surf. Sci. Adv. 6 (2021), https://doi.org/10.1016/j.apsadv.2021.100170.
[91] A. Chaouiki, W. Al Zoubi, Y.G. Ko, Advanced prediction of organic–metal interactions through DFT study and electrochemical displacement approach, J. Magnes. Alloy. (2022), https://doi.org/10.1016/j.jma.2022.04.005.
[92] S.A. Mrani, N. Arrousse, R. Haldhar, A.A. Lahcen, A. Amine, T. Saffaj, S.C. Kim, M. Taleb, In silico approaches for some sulfa drugs as eco-friendly corrosion inhibitors of iron in aqueous medium, Lubricants 10 (2022), https://doi.org/10.3390/lubricants10030043.
[93] J.I. Martínez-Araya, Why is the dual descriptor a more accurate local reactivity descriptor than Fukui functions? J. Math. Chem. 53 (2015) 451–465, https://doi.org/10.1007/s10910-014-0437-7.
[94] R. Atir, A. Idrissi, Z. Elfakir, A. Habsaoui, M.E. Touhami, S. Bouzakraoui, Carbazole-based hole-transport materials for efficient Perovskite solar cells. A computational study, Optik 257 (2022), https://doi.org/10.1016/j.ijleo.2022.168793.